



FEDERAL UNIVERSITY OF PERNAMBUCO
TECHNOLOGY AND GEOSCIENCES CENTER
DEPARTMENT OF ELECTRONICS AND SYSTEMS
GRADUATE PROGRAM IN ELECTRICAL ENGINEERING

BRUNO AGRA KLEINAU

**APPLICATION OF BASE STATION WITH ARRAY OF INTELLIGENT ANTENNAS
IN THE ENERGY DISTRIBUTION SECTOR**

Recife

2022

BRUNO AGRA KLEINAU

**APPLICATION OF BASE STATION WITH ARRAY OF INTELLIGENT ANTENNAS
IN THE ENERGY DISTRIBUTION SECTOR**

Thesis presented to the Graduate Program
in Electrical Engineering of the Federal
University of Pernambuco, as a partial
requirement for the title of Doctor in
Electrical Engineering.

Concentration area: Photonics.

Advisor: Prof. Dr. Marcos Tavares de Melo.

Recife

2022

Catálogo na fonte
Bibliotecário Gabriel Luz / CRB 2222

- K64a Kleinau, Bruno Agra.
Application of base station with array of intelligent antennas in the energy distribution sector / Bruno Agra Kleinau. - 2022.
62 f.: il.
- Orientador: Prof. Dr. Marcos Tavares de Melo.
Tese (Doutorado) – Universidade Federal de Pernambuco. CTG. Programa de Pós-Graduação em Engenharia Elétrica, Recife, 2022.
Inclui referências.
Textos em inglês.
1. Engenharia Elétrica. 2. Sistemas de comando. 3. Arranjos adaptáveis. 4. Arranjos de antenas lineares. 5. Antenas UHF. 6. Estações rádio base. 7. Redes inteligentes. I. Melo, Marcos Tavares de (Orientador). II. Título.
- UFPE
- 621.3 CDD (22. ed.) BCTG 2023 - 84

BRUNO AGRA KLEINAU

**“APPLICATION OF BASE STATION WITH ARRAY OF INTELLIGENT ANTENNAS
IN THE ENERGY DISTRIBUTION SECTOR”**

Thesis presented to the Graduate Program
in Electrical Engineering at the Federal
University of Pernambuco, as a partial
requirement for obtaining the title of Doctor
in Electrical Engineering, in the area of
concentration in Photonics.

Approved: 10 / 11 / 2022.

EXAMINING BOARD

Professor. Dr. Marcos Tavares de Melo (Advisor)
Federal University of Pernambuco (UFPE)

Professor. Dr. Ignácio Llamas-Garro (External Examiner)
Technological Centre of Telecommunications de Catalunya (CTTC) - Barcelona

Professor. Dr. Lauro Rodrigo Gomes da Silva Lourenço Novo (Internal Examiner)
Federal University of Pernambuco (UFPE)

Professor. Dr. Elias Marques Ferreira de Oliveira (External Examiner)
Federal Rural University of Pernambuco (UFRPE)

Professor. Dr. Javier Ontañón Ruiz (External Examiner)
Universidad Nebrija - Madrid.

I dedicate this work to my wife Daniela Wunsch for her patience in understanding my absence during the hours dedicated to this work. I also dedicate this work to my mother Marta Kleinau and my grandmother Ilse Kleinau, because they were my base throughout my education process.

ACKNOWLEDGEMENTS

I thank my family for being responsible for my training as a person and citizen. To my mother, Marta Kleinau for love, support, cheerleading, example and for all the values that have been passed on to me, among them that knowledge is the basis of everything in life. To my late grandmother, who accompanied the beginning of my challenge, but cannot be physically present at that moment, but I'm sure from somewhere she is very happy for this achievement.

To my wife, Daniela. It would be words are very few to express how much I owe you. This achievement is also a little yours, because without your understanding in some moments of absence, this moment would not be possible. Thank you for always being by my side, especially in difficult moments and doubts about whether it would be possible to reconcile this Doctorate with my professional life at Neoenergia. I love you!

My family inherited from my wife, my mother-in-law Zenira and my sister-in-law Vanessa, who always believed that this moment would come. May this achievement be an inspiration to my nephew Peter. Thank you for everything.

I thank my advisor, Professor Marcos Tavares, for having believed in his former undergraduate student and monitor of Electromagnetism 2 in mid-2000. Even in the complicated moments in reconciling professional life with academic life, he was always a counselor and guided me in a very welcoming way and being a permanent supporter throughout my challenge. You allowed and encouraged me to achieve this personal achievement of mine. Professional life has only put off my dream, which is true now.

To research and laboratory colleagues, especially Marcelo Coutinho, Marcelo Alves, Douglas Contente, Jorge, Pedro, Zé Mário, Daniel, Crislane for partnership, exchange of knowledge and relaxing moments in classrooms, congress laboratories or travel. With regard to travel, IMOC in Aveiro, Portugal in 2019 will be marked in my mind for the rest of my life. This trip reminded me of my undergraduate season when I was traveling with fellow students and the lab. Thank you so much for making this challenge a little lighter. You also helped in this conquest.

I thank Neoenergia for the understanding and flexibility i have been given so that I could dedicate myself to the doctorate while performing my professional activities. I thank the R&D program of the National Electric Energy Agency - ANEEL and together with Neoenergia for the financial and logistical support to this project, in collaboration with the Federal University of Pernambuco - UFPE. I thank Ricardo Padilha for the valuable feedbacks of the results

generated during this research that met the R&D project of Intelligent Antennas that he managed within Neoenergia. I also thank the professors and employees of the Graduate Program in Electrical Engineering - PPGEE, for the knowledge and for all the support given, especially in the middle of the COVID-19 pandemic, so that this work would happen and be recognized nationally and internationally.

Thank you all so much!

Bruno Agra Kleinau

"All we have to decide is what to do with the time that is given us." (J. R. R. Tolkien, 1892-1973).

ABSTRACT

The use of Distribution Automation Systems has grown significantly in electricity companies in recent years. The main reason for this is the need to have a smarter network, in order to reduce the time of power interruption. For such applications, communication using Radio Frequency is preferred because this solution is more reliable than 3G/4G and cheaper than fiber optics. In this context, it is of utmost importance to have a more efficient Base Transceiver Station (BTS) that can cover the communication of a larger area. In this work, the mathematical concepts of an intelligent antenna array, as well as the logical operation of an intelligent radiation system controller are presented. Such a system receives as inputs the geographic coordinates of network elements and automatically feeds an intelligent Yagi-Uda antenna array with the appropriate parameters, in order to optimize the radiation pattern in the desired directions. The newly presented model uses a stochastic optimization method to automatically achieve a set of optimal electrical parameters to excite the array, and efficiently direct its beams in a fully controlled way. Thus, the results obtained indicate that the proposed intelligent scheme allows the energy optimization of the antenna system, reducing by 61% the number of BTS needed to cover the same area, when compared to traditional collinear antenna systems.

Keywords: command and control systems; adaptive arrays; linear antenna arrays; UHF antennas; base stations; smart grids.

RESUMO

O uso de Sistemas de Automação da Distribuição tem crescido significativamente nas empresas de energia elétrica nos últimos anos. O principal motivo para isso é a necessidade de uma rede mais inteligente, a fim de reduzir o tempo de interrupção de energia. Para tais aplicações, a comunicação por radiofrequência é preferida porque esta solução é mais confiável do que 3G/4G e mais barata do que fibra óptica. Neste contexto, é de extrema importância ter uma *Base Transceiver Station* (BTS) mais eficiente que possa cobrir a comunicação de uma área maior. Neste trabalho são apresentados os conceitos matemáticos de um arranjo de antenas inteligentes, bem como o funcionamento lógico de um controlador de sistema de radiação inteligente. Tal sistema recebe como entradas as coordenadas geográficas dos elementos da rede e alimenta automaticamente um arranjo de antenas Yagi-Uda inteligente com os parâmetros apropriados, a fim de otimizar o diagrama de radiação nas direções desejadas. O modelo inovador apresentado usa um método de otimização estocástica para atingir automaticamente um conjunto de parâmetros elétricos ideais para excitar o arranjo e direcionar seus feixes de forma totalmente controlada de forma eficiente. Assim, os resultados obtidos indicam que o esquema inteligente proposto permite a otimização energética do sistema de antenas, reduzindo em 61% o número de BTSs necessárias para cobrir a mesma área, quando comparado aos sistemas tradicionais de antenas colineares.

Palavras-chave: sistemas de comando e controle; arranjos adaptáveis; arranjos de antenas lineares, antenas UHF; estações rádio base; redes inteligentes.

LIST OF ILLUSTRATIONS

Figure 1 - Recloser connected to a Yagi-Uda antenna.	19
Figure 2 - Array of Antennas for N isotropic elements.	24
Figure 3 - Model array of 4 Yagi-Uda antennas. Each antenna has 7 elements.	24
Figure 4 - Azimuth diagrams to the Yagi-Uda array in Figure 3, with the objective of aiming the beam to $\theta_0=60^\circ$ (continuous line) and $\theta_0=30^\circ$ (dashed line).	24
Figure 5 - Array of particles in PSO in four different moments of progressive iteration. The red circle indicates the overall optimal location.	26
Figure 6 - Algorithm process flowchart for remote access to HFSS.	28
Figure 7 - Comparison of the gains obtained between the optimization models for the 30° angle.	30
Figure 8 - Comparison of the gains obtained between the optimization models for the 60° angle.	30
Figure 9 - Configuration of the geometry of the intelligent arrays with 360° coverage.	32
Figure 10 - Complete system configuration for three antenna arrays.[6]	33
Figure 11 - Encapsulation of intelligent antenna array control system devices.	36
Figure 12 - Principle of operation of the intelligent array with maximum power density in the desired direction.	37
Figure 13 - Principle of operation of the intelligent array with maximum power density in the desired direction.	37
Figure 14 - Principle of operation of the intelligent array with maximum power density in the desired direction.	38
Figure 15 - Principle of operation of the intelligent array with maximum power density in the desired direction.	38
Figure 16 - Principle of operation of the intelligent array with maximum power density in the desired direction.	39
Figure 17 - Principle of operation of the intelligent array with maximum power density in the desired direction.	39
Figure 18 - Principle of operation of the intelligent array with maximum power density in the desired direction.	40
Figure 19 - Principle of operation of the intelligent array with maximum power density in the desired direction.	40

Figure 20 - Flowchart summarized from the intelligent array optimization process.	41
Figure 21 - Radiation diagrams using the PSO model. (a) 0° - 12.68 dBi, (b) 30° – 10.13 dBi. (c) 60° - 12.76 dBi. (d) 90° - 13.31 dBi.	44
Figure 22 - BTS test and device location satellite view (by Google Earth) showing the angle and distance measured and evaluated by the system.	45
Figure 23 - Radiation diagram for BTS directing the maximum power by the PSO method (14.00 dBi) to the remote test device ($-42^\circ \equiv 318^\circ$). Seen on the azimuthal plane (x -y).	45
Figure 24 - Array of antennas for field measurements.	46
Figure 25 - Receiver System.	46
Figure 26 - Results measured for (a) $\theta_0=10^\circ$, (b) $\theta_0=30^\circ$ and (c) $\theta_0=60^\circ$.	47
Figure 27 - New geometric configuration for intelligent antenna array.	50
Figure 28 - New geometric configuration for intelligent antenna array (superior view).	50
Figure 29 - 7-element Yagi-Uda antenna of the final configuration with grid reflector element. a) Photo present in the datasheet; b) Drawing of the antenna reproduced in the HFSS from its measurements.	51
Figure 30 - Radiation diagram for new configuration with $\theta_0=0^\circ$. Gain of 10.64dBi.	52
Figure 31 - Radiation diagram for new configuration with $\theta_0=15^\circ$. Gain of 12.30dBi.	52
Figure 32 - Radiation diagram for new configuration with $\theta_0=30^\circ$. Gain of 11.33dBi.	53
Figure 33 - Radiation diagram for new configuration with $\theta_0=45^\circ$. Gain of 10.73dBi.	53
Figure 34 - Radiation diagram for new configuration with $\theta_0=60^\circ$. Gain of 12.92dBi.	54
Figure 35 - Radiation diagram for new configuration with $\theta_0=75^\circ$. Gain of 13.95dBi.	54
Figure 36 - Radiation diagram for new configuration with $\theta_0=90^\circ$. Gain of 14.15dBi.	55
Figure 37 - Complete system configuration for two antenna arrays.[6]	55
Figure 38 - Proposal of a model for estimating the parameters of the intelligent array using neural networks.	57

LIST OF TABLES

Table 1 -	Comparison between the Optimization Models Studied.	31
Table 2 -	Radiotechnical characteristics.	34
Table 3 -	Technical characteristics of power divisor.	34
Table 4 -	Technical characteristics of attenuators.	34
Table 5 -	Technical characteristics of the phase shifters.	35
Table 6 -	Technical features of the bidirectional amplifier.	35
Table 7 -	Technical feature of controllable key.	36
Table 8 -	Comparison between intelligent antenna arrays.	48
Table 9 -	Technical characteristics of the antenna used in the intelligent array.	49
Table 10 -	Excitation settings applied to the antennas to obtain the diagrams of Figure 30 to Figure 36.	51

LIST OF ABBREVIATIONS

<i>AF</i>	<i>Array Factor</i>
<i>BTS</i>	<i>Base Transceiver Station</i>
<i>BFC</i>	<i>Beam Former Controller</i>
<i>DoA</i>	<i>Direction of arrival</i>
<i>DGF-FDTD</i>	<i>Discrete Green Functions</i>
<i>ES</i>	<i>Evolution Strategy</i>
<i>GA</i>	<i>Genetic Algorithm</i>
<i>HFSS</i>	<i>High Frequency Structure Simulator (Simulador de Estruturas em Alta Frequência)</i>
<i>IED</i>	<i>Intelligent Electronic Device</i>
<i>MoM</i>	<i>Method of Moments</i>
<i>PSO</i>	<i>Particle Swarm Optimization Method</i>
<i>RF</i>	<i>Radio Frequency</i>
<i>SCADA</i>	<i>Supervisory Control and Data Aquisition</i>
<i>SPDT</i>	<i>Single-Pole-Single-Throw</i>
<i>UHF</i>	<i>Ultra High Frequency</i>

LIST OF SYMBOLS

θ_0	Direction of interest to direct the main lobe of the radiation diagram
N	Number of antenna array elements
d	Distance between antenna array elements
k	Constant propagation of electromagnetic wave
β	Phase of electrical excitation of antenna array elements
a_n	Amplitude of the electrical excitation of the antenna array elements
w	PSO model inertia moment
c_i	Cognitive accelerations of the PSO <i>model</i>
M	Coupling coefficient
Q_e	External Quality Factor
λ_g	Guided wavelength
f_0	Central design frequency applied to antenna array

SUMMARY

1	INTRODUCTION	16
1.1	CHARACTERIZATION AND RELEVANCE OF THE PROBLEM	17
1.2	BIBLIOGRAPHIC REVIEW	19
1.3	MOTIVATION	20
1.4	OBJECTIVES	20
1.5	THESIS STRUCTURE	20
2	360° INTELLIGENT ARRAY MODEL	22
3	OPTIMIZATION OF INTELLIGENT ARRAY PARAMETERS USING PSO MODEL	25
4	COMPARISON OF THE PSO MODEL WITH OTHER PARAMETER OPTIMIZATION MODELS	29
5	OPERATING PRINCIPLE OF THE INTELLIGENT ARRAY OF ANTENNAS AND THEIR CONTROL COMPONENTS	32
6	RESULTS AND DISCUSSIONS	43
6.1	COMPUTATIONAL RESULTS FOR PSO MODEL OPTIMIZATION	43
6.2	COMPLETE SYSTEM SIMULATION	44
6.3	RESULTS MEASURED IN THE FIELD	45
6.4	OPTIMIZATION OF THE GEOMETRIC CONFIGURATION OF THE SMART ARRAY	49
7	CONCLUSIONS	56
7.1	SUGGESTIONS FOR FUTURE WORK	56
7.2	CONTRIBUTIONS AND SCIENTIFIC PRODUCTION	57
7.2.1	Papers published in journals	57
7.2.2	Chapters of published books	58
7.2.3	Papers published in conference editorials	58
7.2.4	Patent application	59
	REFERENCES	60

1 INTRODUCTION

Automation systems have been widely used by the electrical industry in recent years [1]. Currently, there is considerable growth in the number of automated equipment, and radio frequency (RF) communication is one of the main means of remote control used by companies to activate remote devices [2] and [3]. For this application, radio frequency communication is more reliable than 3G/4G systems, due to its independence from outsourced operators, and cheaper than fiber optics systems, being therefore the most viable alternative [4] and [5]. In this context, it is extremely important to have a more efficient BTS, capable of operating distributed devices in a larger area.

Smart antennas use an array whose elements are low gain antennas that are connected by a combined device [6]. Smart antennas can help improve communication system performance by increasing channel capacity and spectrum efficiency, extending range coverage, directing multiple beams to track many devices, and electronically offsetting aperture distortion [7]. For most of the BTS solutions used in the electrical sector, the RF signal is propagated by a collinear array with omnidirectional propagation [8]. In the place where this research generated this work (Pernambuco, Brazil), an array of collinear dipole antennas is used by the electricity distributor (Neoenergia) in each of the Base Transceiver Stations. These Antenna arrays usually generate an omnidirectional radiation pattern with gain of about 6 dBi. By law, the National Telecommunications Agency (ANATEL) restricts the use of radio frequency communication for remote sensing directed to companies providing services of public interest for the frequency ranges of 458 to 460 MHz and 468 to 470 MHz. The first frequency instead of wave band is allocated for transmission of an external station, while the second one is allocated for transmission of the BTS. Using these two bands, the communication protocol between the BTS and the electrical network automation equipment works in a *half-duplex* master-slave manner. Therefore, the BTS communicates with only one device at a time in a pool architecture, and the network device only reports to its BTS when it is questioned.

It is well known that several physical conditions and obstacles, such as distance, vegetation, construction and terrain topology between network devices and BTS can affect link signal quality [5] and [9]. In addition, it can generate interruptions in the radio communication, leaving network devices in shadow regions [10]. To overcome the obstacles of the path and then re-establish the communication link, it is necessary to increase the signal strength, within the allowed power emission limits. Therefore, for optimal use of RF signal generator power, it

is convenient that the maximum power of the radio signal can be intelligently directed to certain areas of interest in a controlled manner.

An alternative to obtain an adjustable directivity of the beams, without the need for mechanical schemes, is the use of intelligent antenna arrays. The use of multiple antenna elements allows such arrays to produce the desired radiation characteristics [11], allowing to point the beams in the desired direction [12] and [13]. Antenna arrays have been widely adopted in several solutions, such as: estimation of the direction of arrival (DOA) for the signal received by the antenna [14] and [15], and concentration of radiation at a predefined point, reducing energy waste in directions where it is not necessary [16].

To increase the efficiency and reach of Base Radio Stations, the theoretical and constructive principles of an RF system that uses an intelligent Yagi-Uda antenna array with electronically controlled 360-degree coverage are presented in this work. The proposed system receives as input the geographic coordinates referring to the locations of the transmitter (BTS) and the network equipment to be activated and, through an embedded mathematical optimization model, is able to automatically control the optimal radiation direction of the power of the RF generator, increasing the range and efficiency of one to Common BTS. The great advantage of this process is that it provides a high-gain concentrated radiation beam in any angular direction of a remote device with which the BTS needs to communicate.

1.1 CHARACTERIZATION AND RELEVANCE OF THE PROBLEM

To increase the efficiency and reach of Base Transceiver Stations, the principles of an intelligent antenna array to maximize radio frequency power are presented in this work.

This thesis proposes the development of an innovative system of intelligent antenna arrays operating in UHF, in the range of 450 to 470 MHz, aimed at the intelligent electrical networks of electricity distributors.

Electricity distribution systems penetrate every region of the country. The advancement of industry, the maintenance of basic services, and the quality of life of the population are closely linked to the continuous and qualitative supply of electricity to the various sectors. In this context, supervisory systems of control and acquisition of SCADA data are employed at different levels to prevent failures and reestablish supply in case of shortages [7].

Once all information about a plant is centralized, it becomes feasible to automate processes such as equipment control and monitoring, plant supervision, command shots, synchronization, variable readings and occurrence recording.

Power distribution networks that cover long distances commonly use SCADA networks, composed of different levels: Equipment (Level 0), IED (Level 1), Remote/Concentrator (Level 2), Communication Network and SCADA (Level 3).

At level 0 are the fixtures that need to be commanded and have information collected remotely. An example of this type of equipment is a recloser, illustrated in Figure 1.

At level 1, device's electrical signals are converted to digital data for command and control. At this level are the transmissions and acquisition and control equipment, which in modern systems are integrated and called IEDs (Intelligent Electronic Device).

Level 2, most commonly used in automation systems in power substations, is composed of one or more IED concentrators (Level 1). In the automation systems architecture on the distribution network, this level may or may not exist.

The communication network is the framework used to transmit information between Level 3 and Level 1, passing or not passing through a Level 2. Within the context of the communication network is that this thesis is based to present a more efficient and innovative system of Radio Frequency.

Finally, Level 3 is the SCADA system, responsible for all supervision, command, control, automatisms and real-time event analysis. It's the human-machine interface mechanism.

Electricity companies, for reliability reasons, massively use their own RF systems. The most common configuration for an BTS is the use of collinear arrays with omnidirectional radiation pattern. BTSs are usually located within a substation, where they can connect to the power company's communication backbone. Remote devices connect to the BTS using antennas that may or may not be directive.

However, in remote regions, such as rural areas or high density of obstacles, such as buildings or vegetation, the signals sent by the substation to the recloser suffer great degradation, reaching the point of not being more readable or even detectable. These regions are called shadow regions. Possible solutions to this problem are the installation of repeater stations or increased transmitter power on the base station and remote stations.



Figure 1 Recloser connected to a Yagi-Uda antenna.

1.2 BIBLIOGRAPHIC REVIEW

Over the past decade wireless communication technology has grown at a formidable rate, creating new and improved services at lower costs. This resulted in an increase in connection duration and number of users [8]. In the case of power distribution companies, users are smart devices integrated into the electricity grid.

As the number of users and the demand for wireless services grow at an exponential rate, the need for larger coverage areas and better transmission quality also increases. Intelligent antenna systems provide a solution to this problem [8].

The traditional way of forming the radiation beams of the RF system is used by the traditional phase displacement method, as shown [8]. This technique enables a controlled domain of beam direction for omnidirectional elements, but does not allow a more assertive domain of beam direction when directive elements such as a Yagi-Uda antenna are used. In addition, the gain is reduced, since the beam generated in the desired direction is also generated in the mirrored direction, as will be shown in the computer simulations later on.

The way to optimize the formation of beams requires the use of computational methods to optimize the parameters of excitation amplitude of each element (weights) and the phases of electrical excitation of each element (phases) [10]. The computational method of optimizing the weight and phase parameters of the most widely used intelligent antenna array is the PSO. The theory and techniques for this more modern approach are in [12] to [16].

The methodology of optimizing the parameters using the PSO model allows you to configure the maximum possible gains in the desired direction, know the angular scan where the array using directive antennas provides maximum gain and define how the combination of intelligent antenna arrays should be composed to allow 360° coverage.

1.3 MOTIVATION

Increasingly, the energy distribution industry is adopting technologies to digitize its networks. The use of proprietary structures with Radio Frequency communication has been shown to be a great advantage, according to the introduction. To optimize investments, ensuring the same coverage area, the use of more efficient Base Radio Stations is necessary.

Conventional Base Radio Stations adopt an omnidirectional radiation standard, radiating all radio power evenly. Since there is a maximum power limit that a station can radiate, so that the same BTS has a higher coverage, it is necessary to make an approach where the power of the radiation diagram can be directed at a certain point of interest.

To optimize the power of an BTS, it is necessary to use intelligent antenna arrays, where by modifying some parameters of the array, it is possible to obtain the maximum gain of the BTS in the desired direction.

With this type of approach, you can have the same coverage using a smaller amount of BTSs in a given region.

1.4 OBJECTIVES

The purpose of this thesis is to propose an electronically controlled intelligent antenna array, so that the radiation diagram of a Base Radio Station has the highest gain in the desired direction. Therefore, the specific objectives of this thesis are:

- a) Analyze and define the control parameters of the intelligent antenna array, in order to obtain the maximum gain in the desired direction;
- b) Define the best mathematical model for optimization of antenna array parameters;
- c) Validate the parameter optimization model by comparing with other approaches and with measured results;
- d) Define the operating model of the control set of the intelligent array of antennas;
- f) Propose the best configuration of the geometry of the intelligent array for a coverage of 360°;

1.5 THESIS STRUCTURE

This work is organized into 7 chapters. Chapter 2 presents the concepts MODEL OF INTELLIGENT ARRAY 360°.

Chapter 3 presents concepts of THE OPTIMIZATION OF INTELLIGENT ARRAY PARAMETERS USING THE PSO MODEL.

Chapter 4 presents the concepts for PSO MODEL COMPARISON WITH OTHER PARAMETER OPTIMIZATION MODELS.

Chapter 5 presents the principle OF OPERATION OF THE INTELLIGENT ARRAY OF ANTENNAS AND THEIR CONTROL COMPONENTS.

Chapter 6 evaluates and presents the results and discussions.

Chapter 7 deals with the conclusions of this thesis. The final considerations and suggestions for further investigations in future work are presented. Finally, the scientific contributions generated in the development of this thesis are presented, listing the publications of the results produced by this work.

2 360° INTELLIGENT ARRAY MODEL

An array of antennas is the name given to the controlled grouping of antennas built to achieve gain and radiation diagram specifications that are unreachable if they are employed by a single antenna. It can be understood, therefore, as a new and complex antenna generated by the combination of a simple set of antennas.

There are 5 possible mechanisms for controlling the radiation pattern of the antenna array [9]:

- 1) Geometric configuration of the array (Linear, Circular, Planar);
- 2) Relative separation between elements;
- 3) Relative diagram of individual elements;
- 4) Range of excitation of each element;
- 5) Phase of electrical excitation of each element;

The first 3 mechanisms are related to geometric factors, while the latter are related to electrical factors. The main objective is to initially define the geometric factors used and then perform intelligent control by changing only the electrical factors.

For the application adopted for energy concessionaires, the best type of array to be applied is linear, because the existing structures are already adapted for this type of antenna array. Other geometries would need physical and operational adaptations of the Operation and Maintenance teams.

It is also important to set the radiation pattern in terms of the antenna element type and the geometric configuration of the array. In punctiform antenna systems (with isotropic source), for example, the total diagram of the array is equal to the diagram of a single antenna element multiplied by the array Factor diagram (AF) [9]. Considering a collinear array with N isotropic elements with the same excitation amplitude and a gradual increase in the electrical phase β of excitation, as shown in Figure 2, the expression for the array factor is given by [8]:

$$AF = 1 + e^{+j(kd \cos \theta + \beta)} + e^{+j2(kd \cos \theta + \beta)} + \dots + e^{+j(N-1)(kd \cos \theta + \beta)}, \quad (1)$$

where d is the spacing between the antennas, k is the constant propagation of electromagnetic wave and β is the phase of electrical excitation of antenna array elements. It can also be written as:

$$AF = \sum_{n=1}^N e^{j(n-1)\psi}, \quad (2)$$

with:

$$\psi = kd \cos \theta + \beta \quad (3)$$

Considering that the maximum array factor occurs when $\psi=0$, regardless of the electrical amplitude applied is uniform or not, the maximum function will occur at an angle θ_0 , according to Equation 3, when:

$$\beta = -kd \cos \theta_0 , \quad (4)$$

where β is the phase of electrical excitation that is gradually applied to the elements [5]. This mathematical method, known as phase-in displacement model [8], allows a control of the desired angle to direct the maximum power to arrays that use omnidirectional elements.

However, when the elements of the array are directive, the application of the phase displacement model is inefficient, as shown in Figure 2.3. These patterns were obtained by attempting to use the mentioned method to direct the radiation pattern of the Yagi-Uda array in Figure 3 to $\theta_0 = 60^\circ$ and $\theta_0 = 30^\circ$. The positive direction of the y-axis (in green color) in Figure 4 points to 90° of these generated azimuth diagrams.

The Ansys HFSS [17] was the electromagnetic simulation software used to design the antenna array presented in Figure 4, as well as to simulate it to obtain its radiation patterns. HFSS is able to use both the Finite Element Method (FEM) [18] and the Moment Method (MoM) [19] to solve electromagnetic problems. In all simulations reported here, a contour condition is selected that uses FEM as a numerical technique to perform its analysis of infinite elements.

It is known that when the element of the array is directive rather than omnidirectional, it provides a greater gain in its oriented physical direction. In this case, to direct the beam to different directions it is necessary to adopt some optimization method to find the appropriate sets of complex excites of the antenna for the array, since the phase displacement model does not apply, given the complexity related to the mutual impedances of the more complex antenna elements. Electromagnetic interference between its elements makes it necessary to use more robust numerical approaches in its modeling.

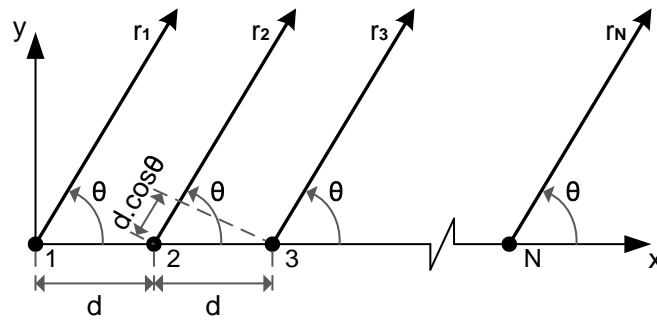


Figure 2 Array of Antennas for N isotropic elements.

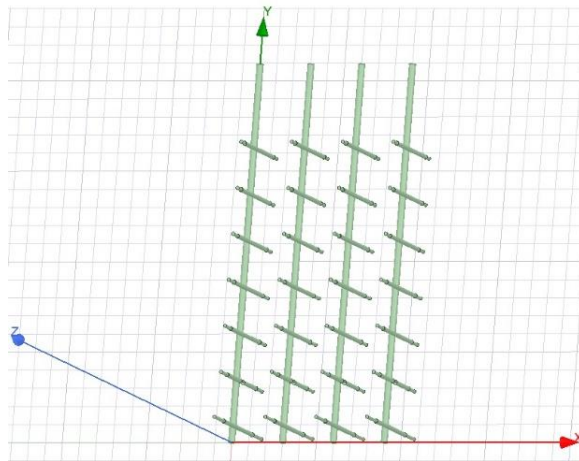


Figure 3 Model array of 4 Yagi-Uda antennas. Each antenna has 7 elements.

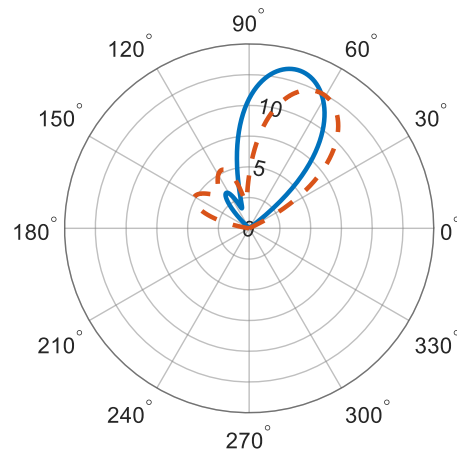


Figure 4 Azimuth diagrams to the Yagi-Uda array in Figure 3, with the objective of aiming the beam to $\theta_0=60^\circ$ (continuous line) and $\theta_0=30^\circ$ (dashed line).

3 OPTIMIZATION OF INTELLIGENT ARRAY PARAMETERS USING PSO MODEL

Due to the need for greater precision, the models of array of Yagi-Uda antennas tend to leave aside the use of concepts of array factor (equations 1 and 2). Being mathematically expressed through induced mutual impedances [10], electromagnetic interferences between their elements make the use of numerical approaches more robust in their modeling almost mandatory. Examples of such numerical costs are the application of the Finite Element Method (FEM) [20], Discrete Green Functions (FDG-FTDT) [12] and Method of Moments (MOM). [11]

To calibrate isotropic antenna array parameters or even Yagi-Uda, the literature has currently been using stochastic optimization techniques [13], [21], [22], [23] and [24]. These stochastic computing methods (e.g., particle swarm optimization) help overcome these complexities in the equation of the model in question [21]. This section discusses the use of *the Particle Swarm Optimization Method* (PSO) with the aim of directing the maximum power beam to θ_0 in the radiation diagram of the Yagi-Uda antenna set, as well as minimizing its secondary lobes. The electrical factors of the array of antennas are treated in the method for these purposes.

Having its initial version developed by R.C. Eberhart [16], the PSO method seeks a parameter adjustment that best measures the mathematical modeling of the system to the restrictions imposed by the chosen objective function. Its concept was initially developed by applying a population-based artificial life (A-life) approach to evolutionary computing in order to optimize continuous nonlinear functions [16]. As an evolutionary self-adaptive algorithm, the advances of its independent agents through iterations emulate the timing of flocked birds or swarm ed bees.

Each possible solution of method, commonly called particle, has its trajectory continuously adjusted toward its best location achieved to date and toward the position of the best particle of the entire swarm at each step of time (generation). The individual influence component of a particle is called the Pbest component (personal best), while the social influence component of the particle set is commonly referred to as Gbest (global best) [16], [25], [26]. Depending on the weight values attached to these components, the speed of each particle can be dominated by its own flight experience or by the flight experience of the other particles [25]. The third and final component used to update the particle position is called the moment component and uses

the previously calculated particle velocity to provide the required inertial factor that the particle needs to mimic a natural fluid movement to traverse the search space [27].

Figure 5 shows an example of the PSO particle array in four different progressive stages during the iteration algorithm process in a search space \mathbb{R}^2 . Dashed arrows indicate the direction of the current movement of particles, while the overall optimal position, which the method is looking for using some objective function, is indicated in red color.

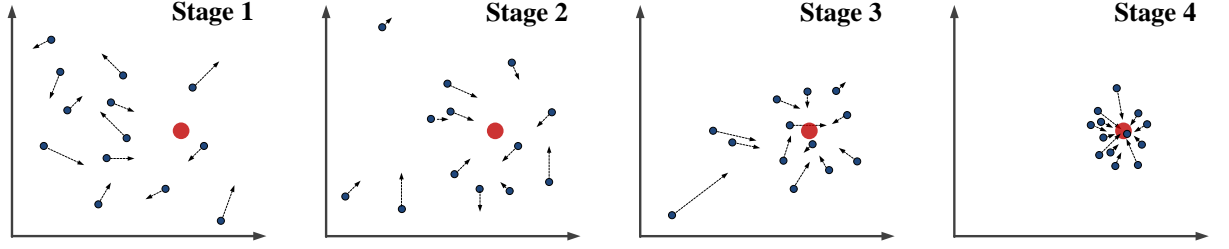


Figure 5 Array of particles in PSO in four different moments of progressive iteration. The red circle indicates the overall optimal location.

In this work, the variables, whose method seeks to find an optimal configuration, are the electrical excites (weights and phases) in the antennas of the array. By this configuration, you expect to get an improved standards diagram. Thus, each PSO particle is a point contained in a subspace $\Omega \subset \mathbb{R}^8$, where four of its components are the power amplitudes ($\in [0; 1]$, in Watts) and the other four are the phase displacements of the signal with which the antennas are fed, $\in [0; 2\pi]$.

The update of the position of each particle is constructed based on the traditional algorithm, found in the literature ([16], [28]), that is:

$$v_i(k+1) = c_1 \cdot rand_1 \cdot (p_{ibest}(k) - x_i(k)) + c_2 \cdot rand_2 \cdot (g_{best}(k) - x_i(k)) + w \cdot v_i(k); \quad (5)$$

$$x_i(k+1) = x_i(k) + v_i(k+1), \quad (6)$$

being w the moment of inertia and c_1 and c_2 the accelerations of cognitive and social dynamics, respectively. These PSO parameters are updated by iteration by:

$$w = (w_{min} - w_{max}) \left(\frac{k}{K_{max}} \right)^2 - w_{max}; \quad (7)$$

$$c_1 = c_{1max} - (c_{1max} - c_{1min}) \cdot \frac{k}{K_{max}}; \quad (8)$$

$$c_2 = c_{2max} - (c_{2max} - c_{2min}) \cdot \frac{k}{K_{max}}, \quad (9)$$

while the calculated maximum speed is maintained, by means of saturation, in the range $[-v_{max}, v_{max}]$, with:

$$v_{max} = \left(K_v - \left(k/K_{max} \right)^p \right) V_{max}, \quad (10)$$

where k is the numeric value of the current iteration and K_{max} is the proposed total number of iterations. W_{min} , W_{max} , C_{1max} , C_{1min} , C_{2max} , C_{2min} , K_v , p and V_{max} are positive constants adjusted by trial and error, following the initial selection criteria pointed out by [25], [29], [30]. The reflector condition is used as a contour manipulation condition for the proposed optimization. Reflective, invisible and damping boundary techniques are three promising methods when used in PSO to deal with antenna calibration problems [26], [31], [32].

The objective function used in the PSO contains two components. The first maximizes the value of the diagram at the angular position θ_0 , where you want to maximize the power. The second, of lower weight, minimizes the secondary lobes [27], [33] in positions above 0 dBi, which rectifies some adverse events resulting from the first. Each particle has its components injected into the mathematical model of the antenna array and the errors resulting from these two objectives are calculated and summed. The resulting value is then used as a performance meter for the current particle position.

To find the secondary lobes in the patterns diagram generated from the position of each particle, a lobe detector code is written. It is capable of returning the angular positions in which the lobes of interest are located, namely those greater than 0 dBi. By these positions are taken the respective values in dBi in the diagram. Then these error values are summed up, resulting in the component of the second weightless objective function. Lobes that have position near the desired lobe are not computed in this sum, that is, those angularly closer to 4° of θ_0 . This approach allows the pattern to become in place in a configuration, within a confidence interval that minimizes the error.

The applied PSO algorithm was written in Python [34] and used by remote access to HFSS [17]. For each iteration of the algorithm, the current position of each particle is inserted into the HFSS project as its electrical excites, using the appropriate Python packages and modules. Soon after, the resulting radiation patterns are extracted from the HFSS by the algorithm, exported as a table containing its set of points. Then, the objective function uses these tables to punctuate

each particle position as mentioned above. Figure 6 presents a flowchart that shows the generic process of the algorithm remotely accessing HFSS to punctuate the position of a particle.

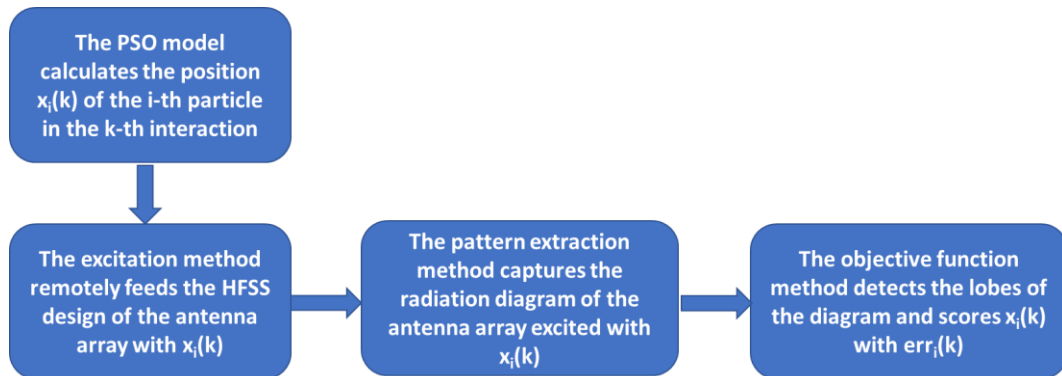


Figure 6 Algorithm process flowchart for remote access to HFSS.

4 COMPARISON OF THE PSO MODEL WITH OTHER PARAMETER OPTIMIZATION MODELS

The first objective of this research was to determine a methodology for estimating the electrical parameters of the intelligent antenna array. This research is an evolution of a first stage of a research and development project carried out between Neoenergia and UFPE. In the first stage of the project there was no methodology directed to the estimation of the excitation parameters of the intelligent antenna array, which did not guarantee the application of optimized excitation parameters. The estimated time of these parameters was also not well defined before. Thus, there was no methodology that ensured that the applied parameters were optimized to obtain the maximum power density of the RF signal in the desired direction. After a bibliographical research of similar applications in other different areas of the electricity sector, three different methods were selected for comparison and determination of the most efficient.

As a way to validate the most efficient optimization model, the PSO model, already covered in chapter 3, had its results obtained compared to two other optimization models.

One of the models used for the comparison was the Evolution Strategy. The Evolution Strategy optimization technique was created in the early 1960s and further developed in the 1970s.

Evolution strategies use problem-dependent natural representations, and mainly mutation and selection, as search operators. In common with evolutionary algorithms, operators are applied in a loop. An iteration of the loop is called generation. The generation sequence is continued until an end criterion is met.

The other optimization model tested was the Genetic Algorithm (GA). In a Genetic Algorithm, a population of candidate solutions (called individuals, creatures, organisms, or phenotypes) for an optimization problem evolves into better solutions. Each candidate solution has a set of properties (its chromosomes or genotypes) that can be mutated and altered; traditionally, solutions are represented in binary as *strings of* 0s and 1s, but other encodings are also possible.

In computer science and operational research, a Genetic Algorithm is a metaheuristic inspired by the natural selection process that belongs to the larger class of evolutionary algorithms. Genetic algorithms are commonly used to generate high-quality solutions for optimization and search problems, recounting operators in which they are involved in the biological process, such as mutation, crossing and selection. Some examples of Genetic

Algorithms applications include decision tree optimization for better performance, sudoku puzzle solving, hyperparameter optimization.

Simulating the models to obtain the best parameters comparing the PSO, ES and GA models, the results of Figure 7 and Figure 8 were obtained.

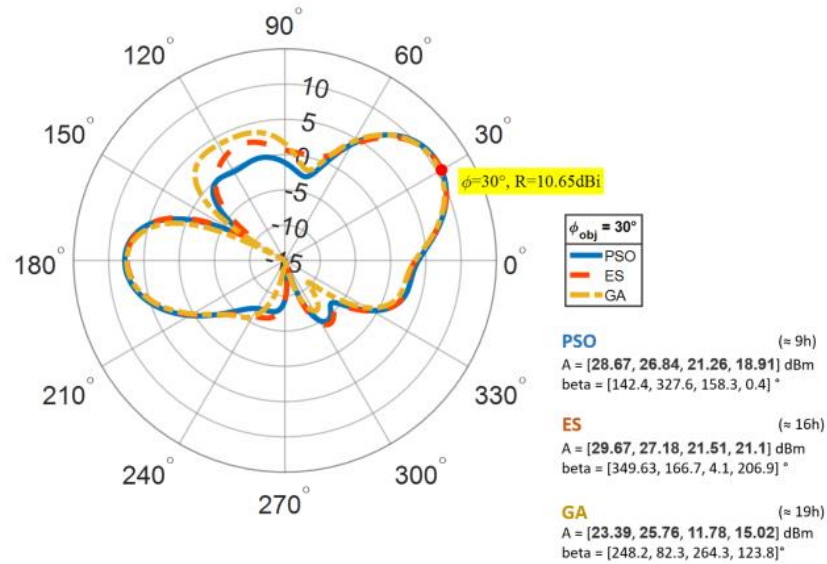


Figure 7 Comparison of the gains obtained between the optimization models for the 30° angle.

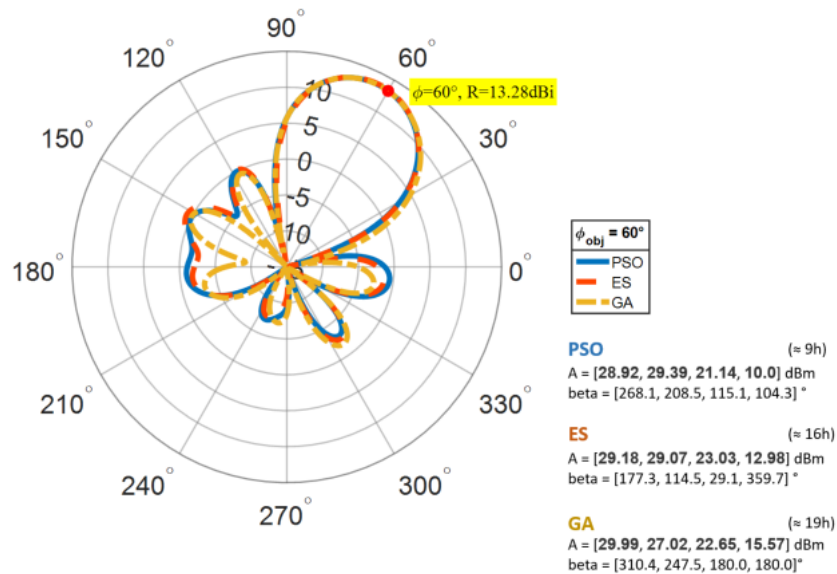


Figure 8 Comparison of the gains obtained between the optimization models for the 60° angle.

According to the results of Figure 7 and Figure 8, all 3 parameter optimization models converge to a radiation diagram with maximum gain in the desired direction. However, the PSO model has a shorter convergence time than the other models. While the PSO takes about 9 hours to get the desired parameters, the ES and GA optimization models take 16 and 19 hours of simulation respectively.

In addition to the PSO model having better computational performance, it has several references in applications for setting parameters of intelligent antenna arrays.

Table 1 summarizes the operational performance of the 3 optimization models studied.

Table 1 Comparison between the Optimization Models Studied.

Optimization Model	RF Signal Gain Targeting Null (θ_0)	Gain	Model Optimization Time
PSO	30°	10.65 dBi	~9 hours
	60°	13.28 dBi	
ES	30°	10.65 dBi	~16 hours
	60°	13.28 dBi	
GA	30°	10.65 dBi	~19 hours
	60°	13.28 dBi	

5 OPERATING PRINCIPLE OF THE INTELLIGENT ARRAY OF ANTENNAS AND THEIR CONTROL COMPONENTS

For the control of the intelligent array of antennas, it is necessary to use electronically controlled RF devices and intelligent control systems. In this chapter will be presented the principle of operation of the array of intelligent antennas, as well as their components.

For the final composition of the BTS with a coverage of 360° , it is necessary to evaluate the coverage of an intelligent array operating individually. Later, in the results obtained, it will be shown that the intelligent array with 4 parallel Yagi antennas has a coverage of 120° for a gain greater than 10dBi.

The complete system of intelligent arrays consists of 3 arrays of antennas distributed in 360° with a spacing of 120° between each, as shown in Figure 9.

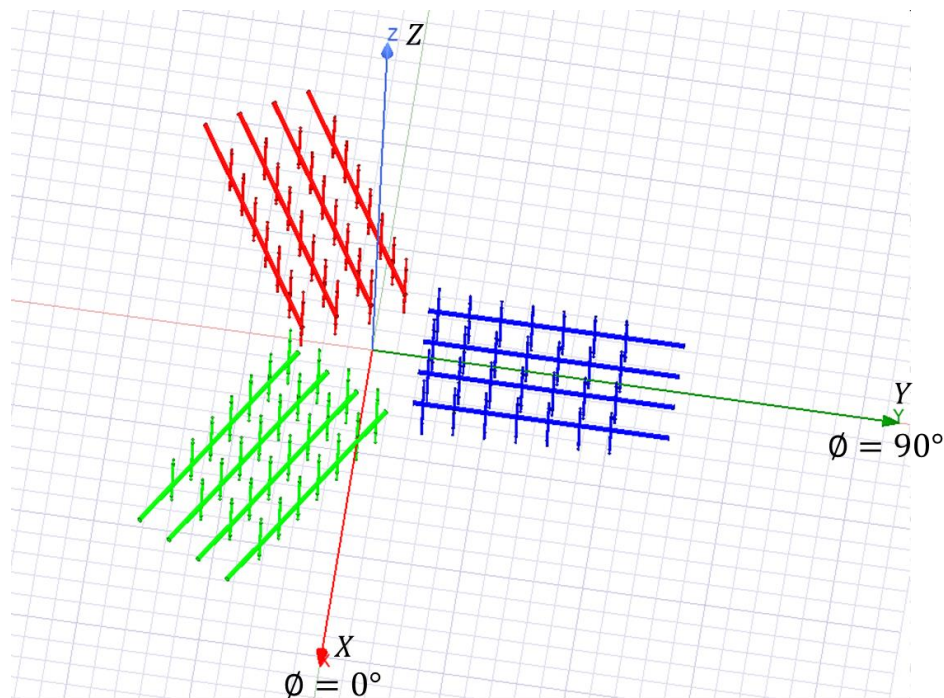


Figure 9 Configuration of the geometry of the intelligent arrays with 360° coverage.

Each of the 3 intelligent arrays has an individual control of excitation amplitude and the electrical excitation phase for each individual element of the arrays. An Intelligent Array Controller (IAC) is responsible for all processing intelligence in order to define the parameters that will excite the arrays so that the maximum gain is pointed to the desired direction.

The geographic coordinates of the BTS, where the smart antenna arrays are located, as well as the geographic coordinates of the remote smart devices to be controlled can be IAC input

parameters. With the information on the location of the BTS and devices, the controller converts the geographic coordinates into polar coordinates identifying the angle θ_0 . This angle corresponds to the relative direction of the device intended to receive the maximum power from the BTS. Figure 10 illustrates the complete control system. For directing the power of the RF signal from the generator in each of the antenna arrays, a SPDT switch is used, which is part of the IAC. The θ_0 angle can also be previously calculated and the information entered into the IAC for better processing performance.

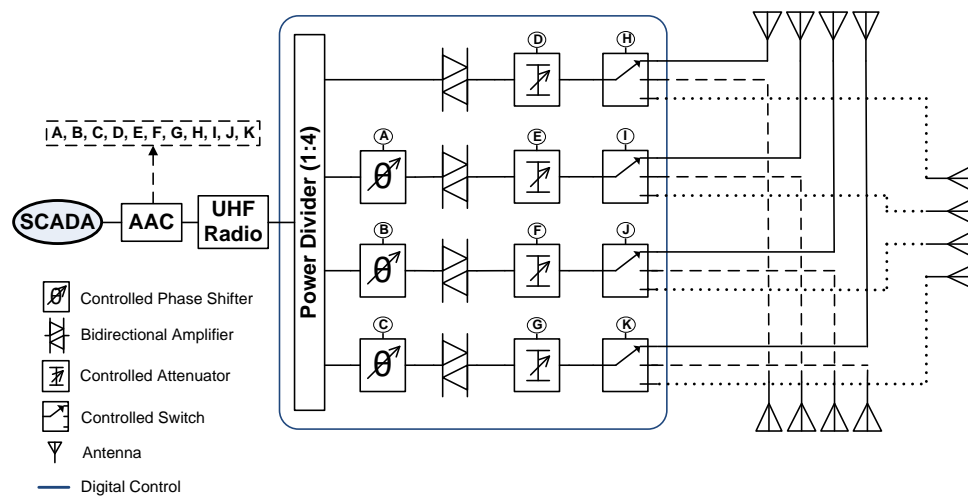


Figure 10 Complete system configuration for three antenna arrays.[6]

The complete configuration of the antenna array control system consists of the following devices:

IOC (Integrated Operations Center) / SCADA- Represents the control system that will select the device that will be read by the Intelligent Array of Antennas. The commands are sent by the SCADA system (Supervisory Control and Data Acquisition), where the BTS and Remote Devices are configured.

IAC – It is the Intelligent Array Controller, where the entire control system is located to set the control parameters (excitation amplitude and the electrical excitation phase) to direct the maximum power of the Intelligent Array at the angle of interest.

UHF Radio - Device responsible for generating the RF signal that will power the Intelligent Array. More technical details are described in Table 2.

Table 2 Radiotechnical characteristics.

Features	Min.	Tip.	Max.	Unit
Operating Range	406		470	MHz
Output impedance		50		Ω
Output power	30		40	dBm

Power Splitter - Device used to collect a control signal to determine the transmission and reception status of the two-way amplifiers. More technical details are described in Table 3.

Table 3 Technical characteristics of power divisor.

Features	Min.	Tip.	Max.	Unit
Operating Range	350		1000	MHz
Input Characteristic Impedance (SMA)		50		Ω
Split factor		1:4 (6dB)		
VSWR	1,5:1			
Loss of insertion			7	dB
Insulation between output ports	15			dB
Maximum operating power			30	W

Controllable Attenuators and Phase Shifters – Electronically controlled devices for the purpose of parameterizing the excitation amplitudes and electrical excitation phases of the elements of each intelligent array. More technical details are described in Table 4 and Table 5.

Table 4 Technical characteristics of attenuators.

Features	Min.	Tip.	Max.	Unit
Operating Range	DC		2000	MHz
Input Characteristic Impedance (N)		50		Ω
Attenuation	6		120	dB
Phase difference by attenuation		1		%dB
Maximum operating power (average)			5	W
VSWR			1,5:1	

Table 5 Technical characteristics of the phase shifters.

Features	Min.	Tip.	Max.	Unit
Operating Range	400		500	MHz
Input Characteristic Impedance (SMA)		50		Ω
Minimum phase increment	1,41			°
Maximum lag			360	°
VSWR	2:1			
Insertion loss			6	dB
Maximum operating power			100	mW
Control voltage		± 5		V
Control connector		Micro D15		

Bidirectional Amplifiers - Electronically controlled devices for the purpose of defining transmission and reception modes. More technical details are described in Table 6.

Table 6 Technical features of the bidirectional amplifier.

Features	Functionality	Min.	Tip.	Max.	Unit
Operating Range		30		2700	MHz
Input Impedance			50		Ω
Gain	Transmitter			36	dB
Loss of return		-12		15	dB
Switching time			1		μsec
DC supply voltage		12		30	V
Operating Range		30		2700	MHz
Input Impedance			50		Ω
Gain	Receiver			30	dB
Loss of return		-10		12	dB
Compression point 1dB			15		dBm

Controllable Switch – Electronically controlled devices for the purpose of selecting the intelligent array of the set of arrays that should receive the parameterizations of the excitation amplitudes and the phases of electrical excitation. More technical details are described in Table 7.

Table 7 Technical feature of controllable key.

Features	Min.	Tip.	Max.	Unit
Operating Range	DC		26	GHz
Input Impedance		50		Ω
VSWR	1,5:1			
Loss of insertion			0,2	dB
Insulation	70			dB
Power supply			12/300	V/mA

The devices that make up the system in Figure 10 were packaged in a standard 19" cabinet, shown in Figure 11.

**Figure 11** Encapsulation of intelligent antenna array control system devices.

The ultimate goal of the smart array is for the BTS to scan all automated devices according to the SCADA system read and collect parameterization shown in Figure 10. Once with the angles where the maximum power density must be directed, the optimized parameters must be inserted in the attenuators and phase shifters of the set of Figure 10.

Figure 12 to Figure 19 show how the 360° coverage principle of the recloser, directing the maximum power density in the desired direction.

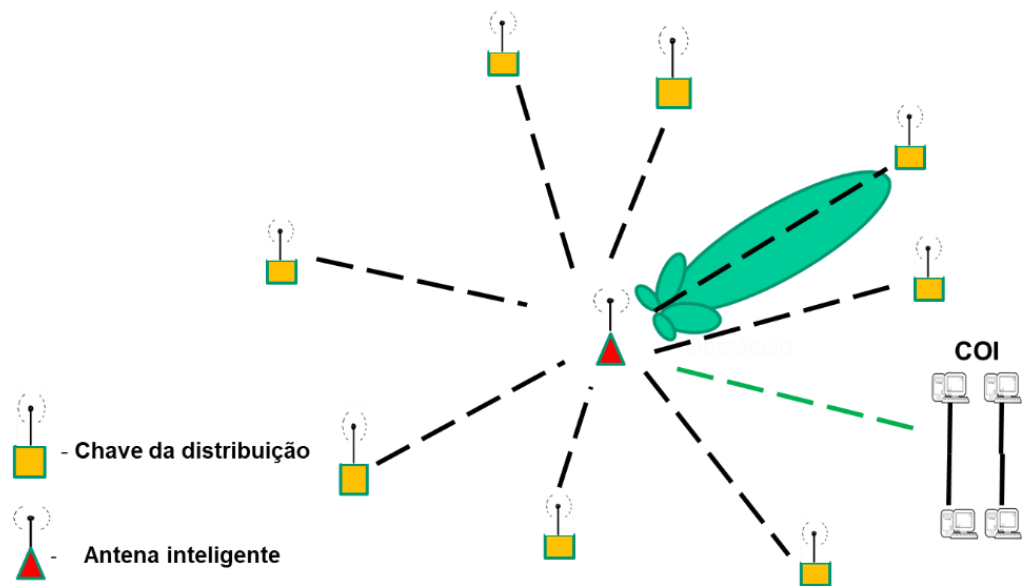


Figure 12 Principle of operation of the intelligent array with maximum power density in the desired direction.

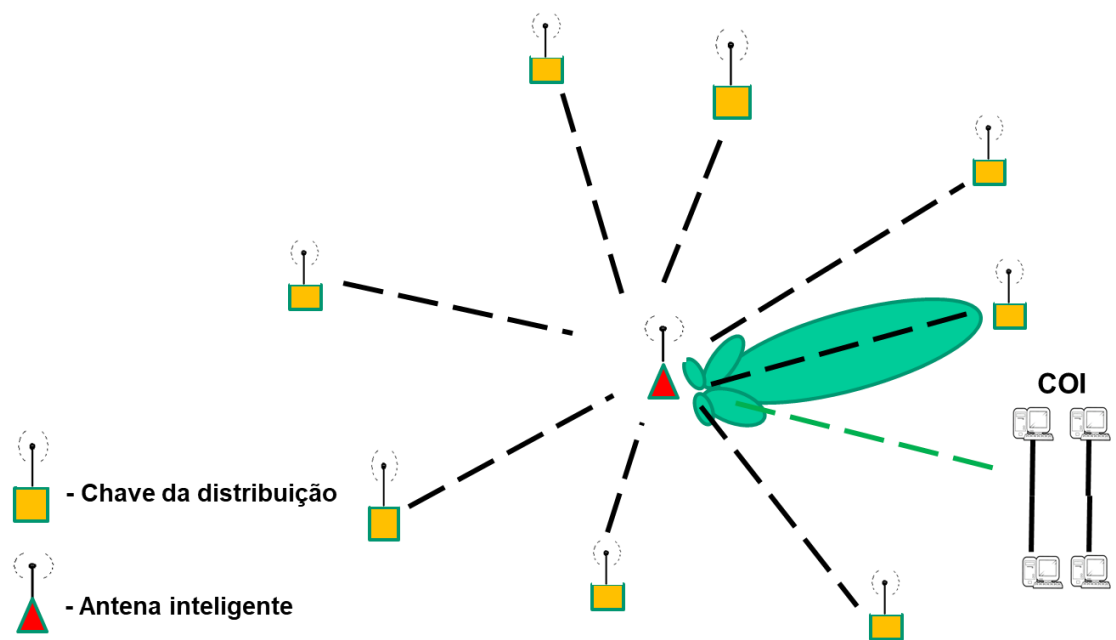


Figure 13 Principle of operation of the intelligent array with maximum power density in the desired direction.

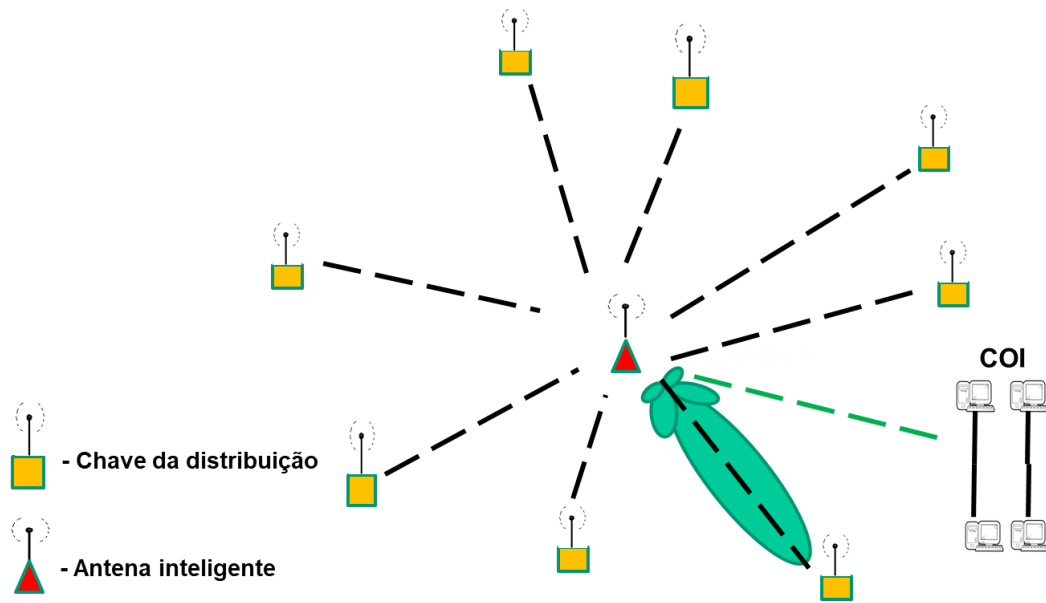


Figure 14 Principle of operation of the intelligent array with maximum power density in the desired direction.

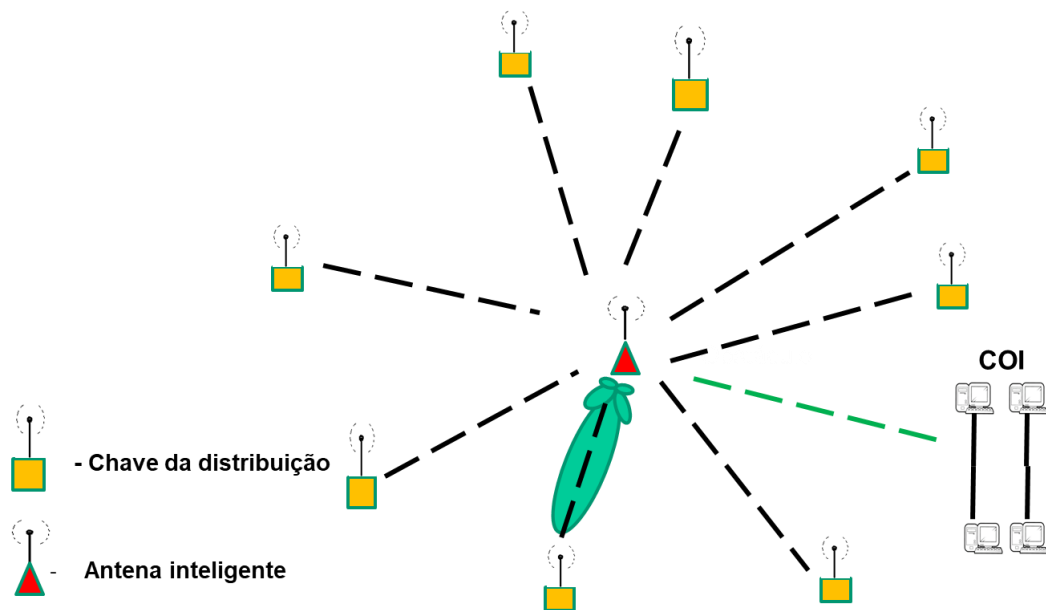


Figure 15 Principle of operation of the intelligent array with maximum power density in the desired direction.

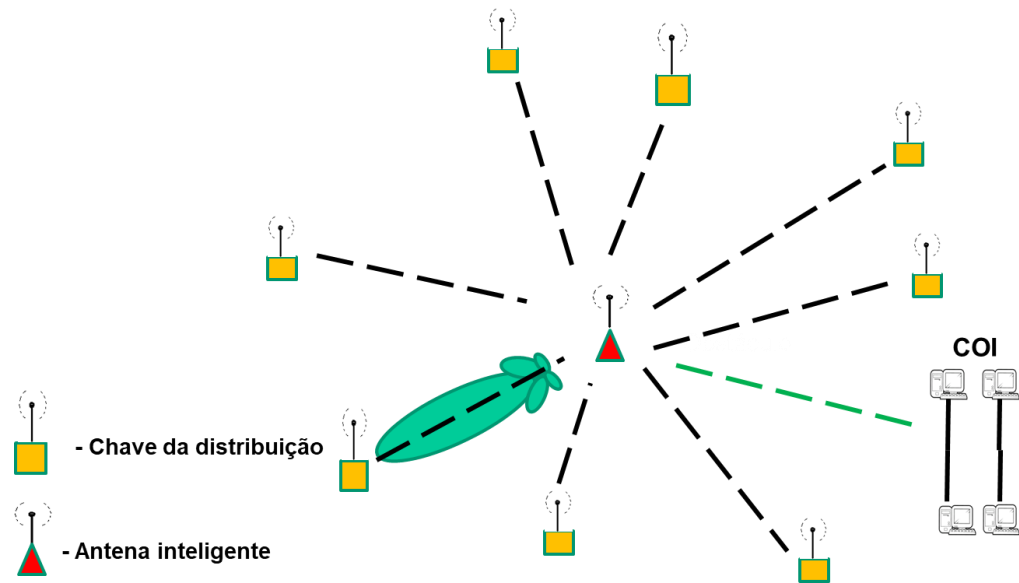


Figure 16 Principle of operation of the intelligent array with maximum power density in the desired direction.

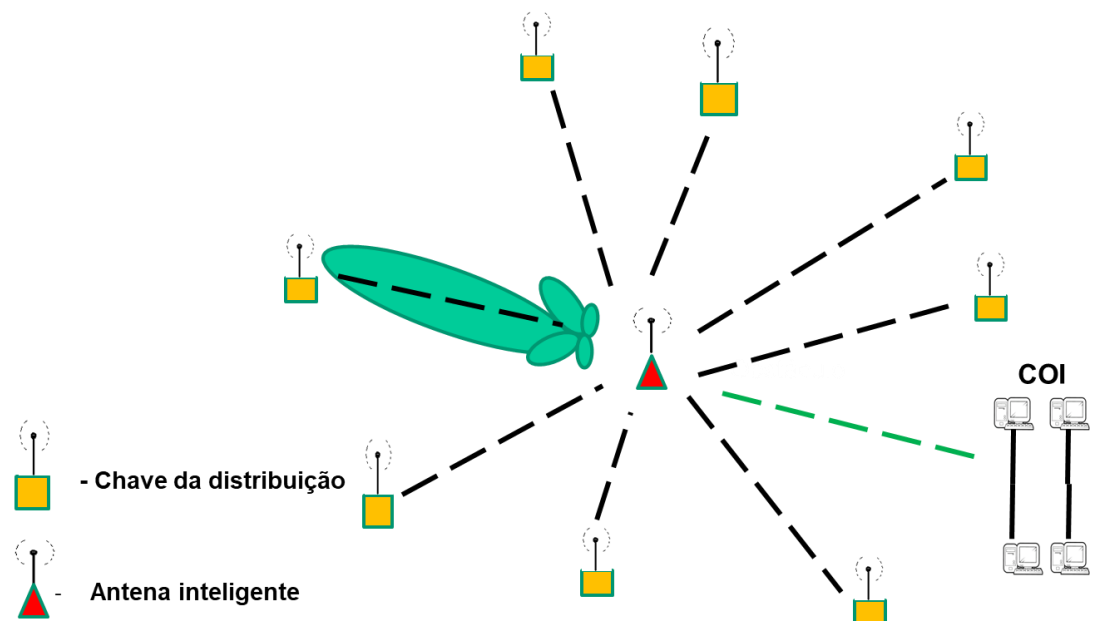


Figure 17 Principle of operation of the intelligent array with maximum power density in the desired direction.

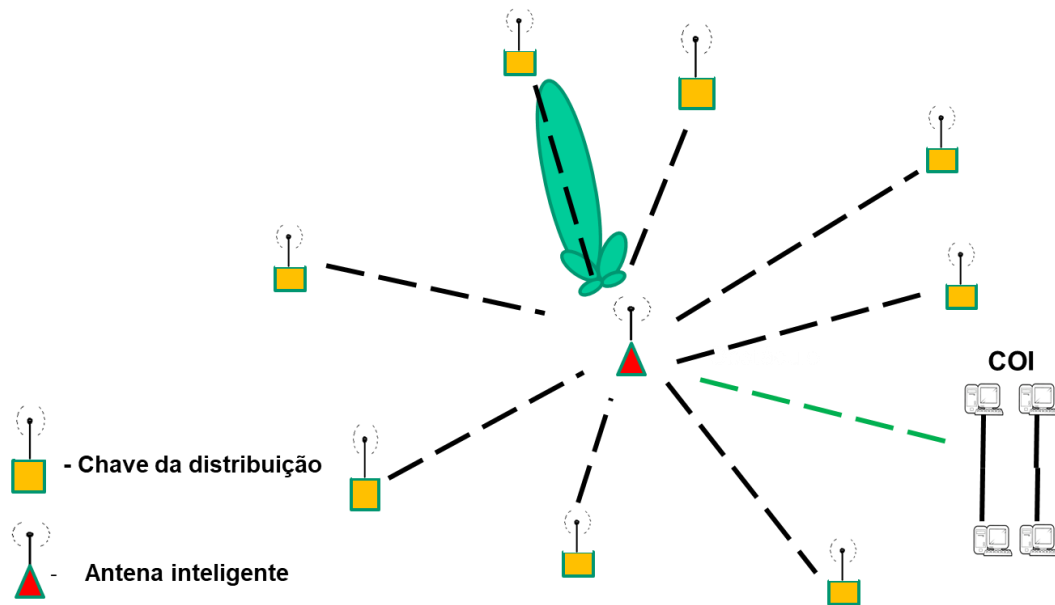


Figure 18 Principle of operation of the intelligent array with maximum power density in the desired direction.

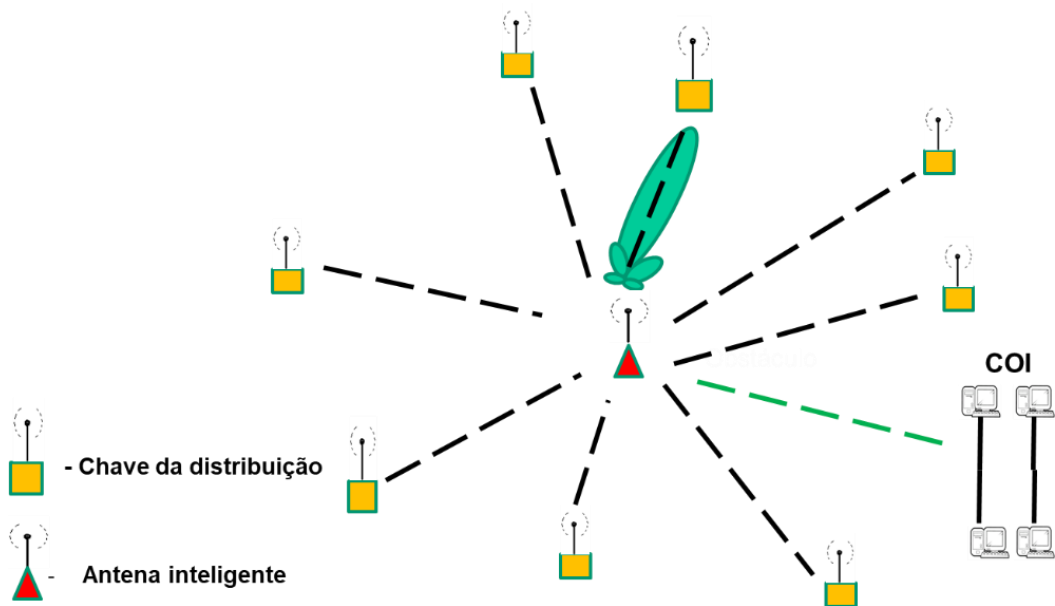


Figure 19 Principle of operation of the intelligent array with maximum power density in the desired direction.

For the determination of the angle θ_0 having the location information of the BTS and the devices, the methodology of conversion of geographic coordinates into polar coordinates is adopted. Figure 20 shows the flowchart of the process of optimizing the intelligent array of antennas, having as input the geographical coordinates of the BTS and the device that wants to direct the maximum power of the RF signal.

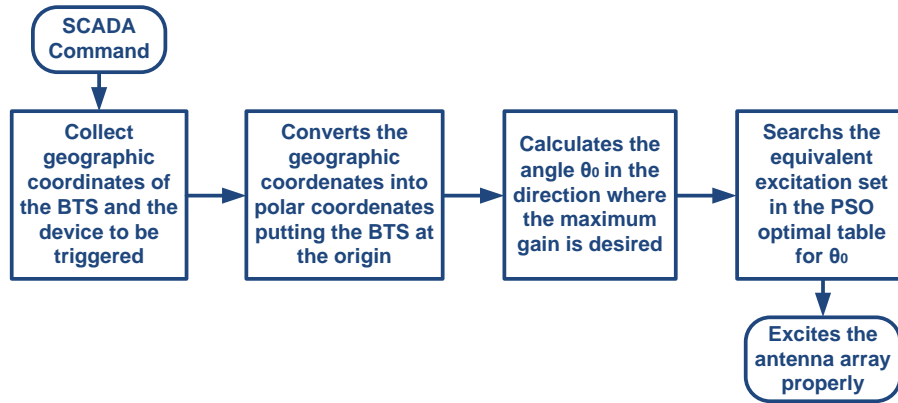


Figure 20 Flowchart summarized from the intelligent array optimization process.

For the conversion of geographic coordinates at angle θ_0 , the geographic locations (latitude, longitude) of each element of the system must be converted into a spherical coordinate system (Θ, φ) . The BTS is located in a position equivalent to the point $(0,0)$ of this spherical coordinate system, and the reference of the angles is the vector that points in the normal direction of the antenna array.

Considering an element in the geographical position (lat, lon) , the conversion to the system (Θ, φ) is given by:

$$\theta = \frac{\pi}{2} - \frac{\pi lat}{180}; \text{ and } \varphi = \begin{cases} \pi \cdot \frac{lon}{180}, & \text{if } lon > 0; \\ 2\pi + \pi \cdot \frac{lon}{180}, & \text{otherwise.} \end{cases} \quad (11)$$

Whereas the BTS coordinates are $(\Theta_{BTS}, \varphi_{BTS})$ and that the Earth's R radius remains approximately constant between small distances on its surface, the repositioning of the other devices $(\Theta_{dev}, \varphi_{dev})$ in the system (x, y, z) so that the BTS is in the position equivalent to the geographical point $(lat = 0, long = 0)$ is given by:

$$\begin{bmatrix} x \\ y \\ z \end{bmatrix} = [A] \cdot \begin{bmatrix} R \cos \varphi_{dev} \sin \theta_{dev} \\ R \sin \varphi_{dev} \sin \theta_{dev} \\ R \cos \theta_{dev} \end{bmatrix}, \quad (12)$$

With $[A]$ equal to:

$$\begin{bmatrix} \sin(\theta_{BTS})\cos(\varphi_{BTS}) & \sin(\theta_{BTS})\sin(\varphi_{BTS}) & \cos(\theta_{BTS}) \\ -\sin(\varphi_{BTS}) & \cos(\varphi_{BTS}) & 0 \\ -\cos(\theta_{BTS})\cos(\varphi_{BTS}) & -\cos(\theta_{BTS})\sin(\varphi_{BTS}) & \sin(\theta_{BTS}) \end{bmatrix}. \quad (13)$$

Finally, considering vector V_r as the zero reference direction of the antenna array, the δ angle between V_r and the device positioned at point $P_{dev} = (x, y, z)$ is given by:

$$\delta = \cos^{-1} \left(\frac{V_r \cdot P_{dev}}{\|V_r\| \|P_{dev}\|} \right). \quad (14)$$

The control parameters of the array for the geometric configurations of the array are predefined and the gain and direction of the radiation diagram are electronically controlled by the IAC, varying the excitation amplitudes and the phases of electrical excitation.

6 RESULTS AND DISCUSSIONS

In this chapter, the simulated and measured results are presented for the optimization model of the electrical parameters of the intelligent array of antennas. The simulations and measurements are performed for one of 3 arrays of the complete set of arrays shown in Figure 9.

6.1 COMPUTATIONAL RESULTS FOR PSO MODEL OPTIMIZATION

Attempts to adapt Equation 1 to the mathematical model of the Yagi-Uda antenna and all its electromagnetic interferences end up generating a high computational cost. This cost includes the need to solve non-elementary integral equations of induced impedances between model components [10], [11], [12], [20]. In addition, in some cases there is no direct access to the modeling applied by the simulation software and its numerical approximations. That said, it would be relatively complex to determine an efficient balance between computational cost and mathematical precision in these mathematical adaptations of Equation 1. It should also be commented that the stochastic method uses the software model's own responses in its optimization, making it easily adapted to the particularities of electromagnetic interferences of the system that are calculated by its platform. This indicates efficiency for different simulation software, within its own different levels of numerical accuracy delivered.

The constructive geometry of the proposed intelligent array, based on the angular range of a 120° azimuthal sector ensured by the PSO, consists of the combination of 3 intelligent collinear arrays, operating independently. The 3 arrays are mirrored and each covers independently 120° , with a total coverage of 360° , as shown in Figure 9.

Numerical simulations were made in HFSS [17] and Python [34] for settings 0° (Broadside), 30° , 60° and 90° (End-Fire) using PSO. Figure 21 shows the results of the radiation diagram of the model of three arrays of antennas. The positive direction of the y-axis in Figure 9 points to 90° of the patterns in Figure 21. For all diagrams shown in this figure, the directivity is given in dBi for a frequency of 459,438 MHz.

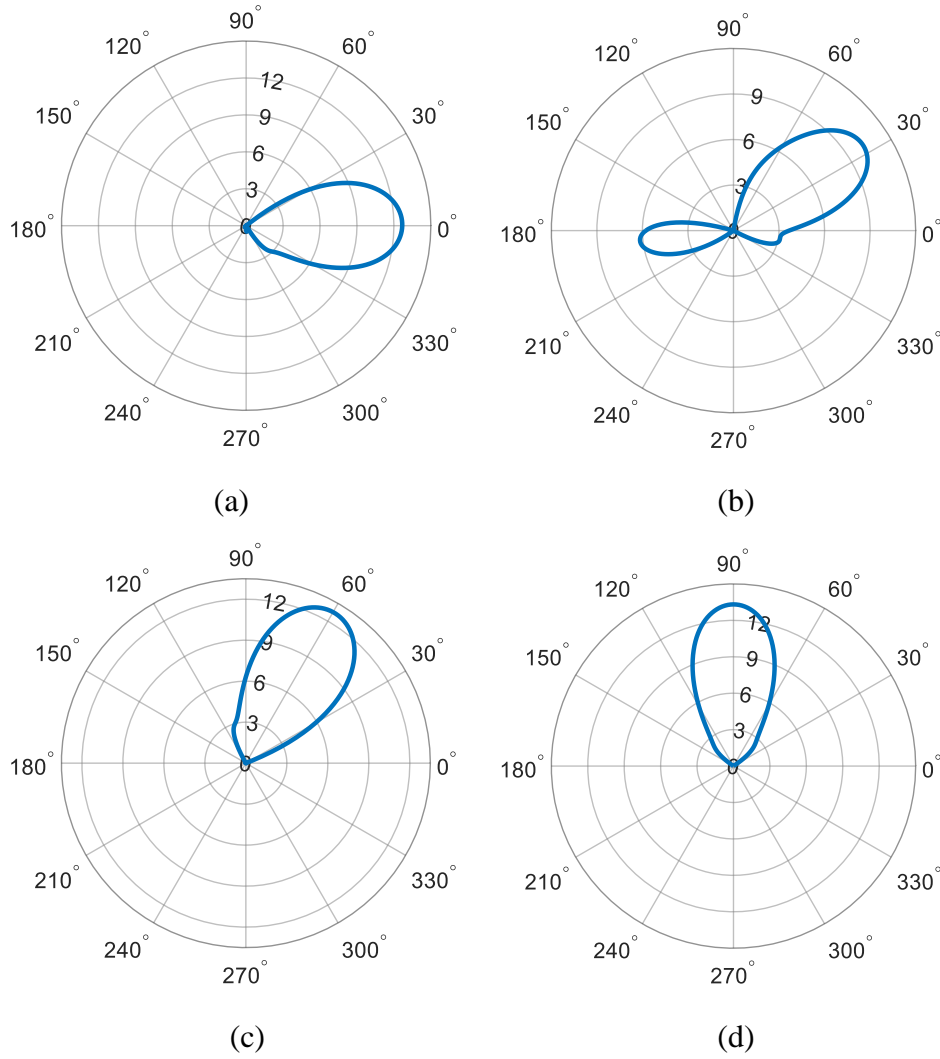


Figure 21 Radiation diagrams using the PSO model. (a) 0° - 12.68 dBi, (b) 30° – 10.13 dBi. (c) 60° - 12.76 dBi. (d) 90° - 13.31 dBi.

6.2 COMPLETE SYSTEM SIMULATION

The calculation of the angle and distance of the device in relation to the BTS can be seen in Figure 22. The actual coordinates of an BTS ($8^{\circ}11'51.4''\text{S}$, $35^{\circ}34'39.7''\text{W}$) and a device ($8^{\circ}12'51.7''\text{S}$, $35^{\circ}33'30.6''\text{W}$) located in the city of Gravatá, State of Pernambuco, Brazil, were used. Comparing the calculated result with the one measured with Google Earth, it can be observed that the system presents a relative error of less than 0.2% in relation to the relative position of the elements.

The angle calculated in the conversion model for the BTS and one of the devices is $\theta_0 = -42^{\circ}$. The result of the complete system is shown in Figure 22. The mathematical model presented in equations 11 to 14 was used.

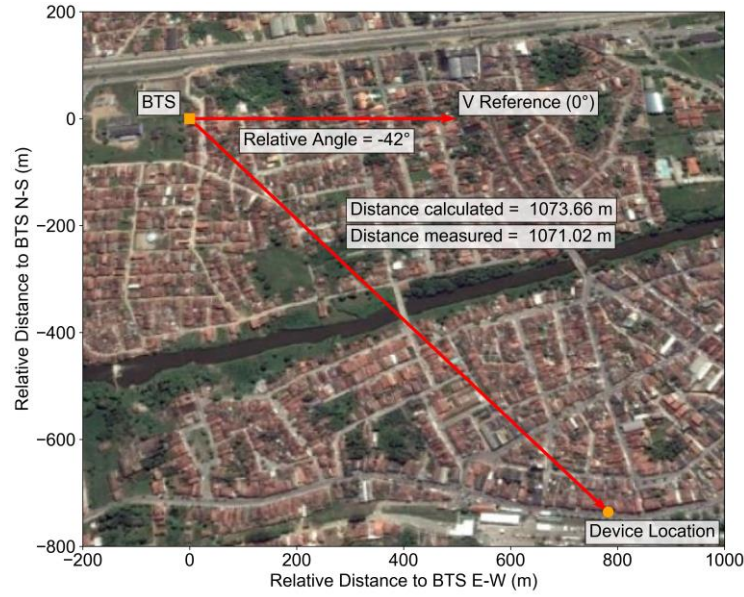


Figure 22 BTS test and device location satellite view (by Google Earth) showing the angle and distance measured and evaluated by the system.

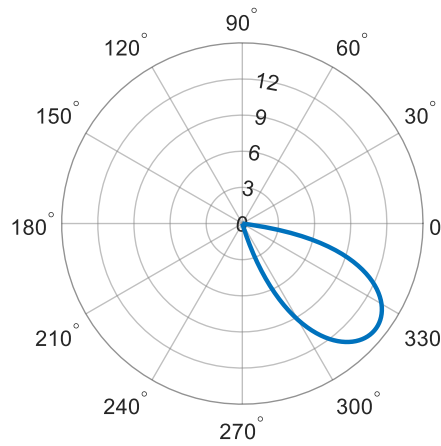


Figure 23 Radiation diagram for BTS directing the maximum power by the PSO method (14.00 dBi) to the remote test device ($-42^\circ \equiv 318^\circ$). Seen on the azimuthal plane (x -y).

6.3 RESULTS MEASURED IN THE FIELD

To validate the simulated mathematical model, the Antenna Array of Figure 24 was assembled with the 4 Yagi-Uda antennas of the numerical simulations and the receiver antenna in Figure 25 was used to measure the power of the Antenna Array. The Array of Antennas was rotated around its shaft every 10 degrees to read the power on the receiver and thus build the array radiation diagram [19]. Measurements were performed considering the array parameters for angles $\theta_0=10^\circ$, $\theta_0=30^\circ$ and $\theta_0=60^\circ$. A radio was connected to the Antenna Array and the

receiving antenna and the RSSI (Received Signal Strength Indication in dBm) of the receiving antenna was captured via SSH protocol (Secure Shell). Commercial attenuators and phase shifters were used to control signal amplitude and phase.

Measurement parameters:

- Transmitted Array Frequency: 459 MHz
- Distance between fixed antenna and matrix: 15.3 m (between masts, greater than distant field distance)
- Antenna height: 2 m (from ground)



Figure 24 Array of antennas for field measurements.



Figure 25 Receiver System.

Figure 26 shows the comparison between the simulated normalized radiation diagram and the measured one. The results are in good agreement. The differences observed between the measured and simulated responses are due to the imperfect parallelism of the antennae and small errors of phase and amplitude of the signals that feed the array of the experimental setup, compared to those calculated. However, the maximum radiation angle accurately corresponds to the desired positions of the elements, which demonstrates the system's ability to automatically find the best set of parameters to excite the Antenna Array and intelligently control the radiation diagram, optimizing the RF signal of the BTS transmitter radio.

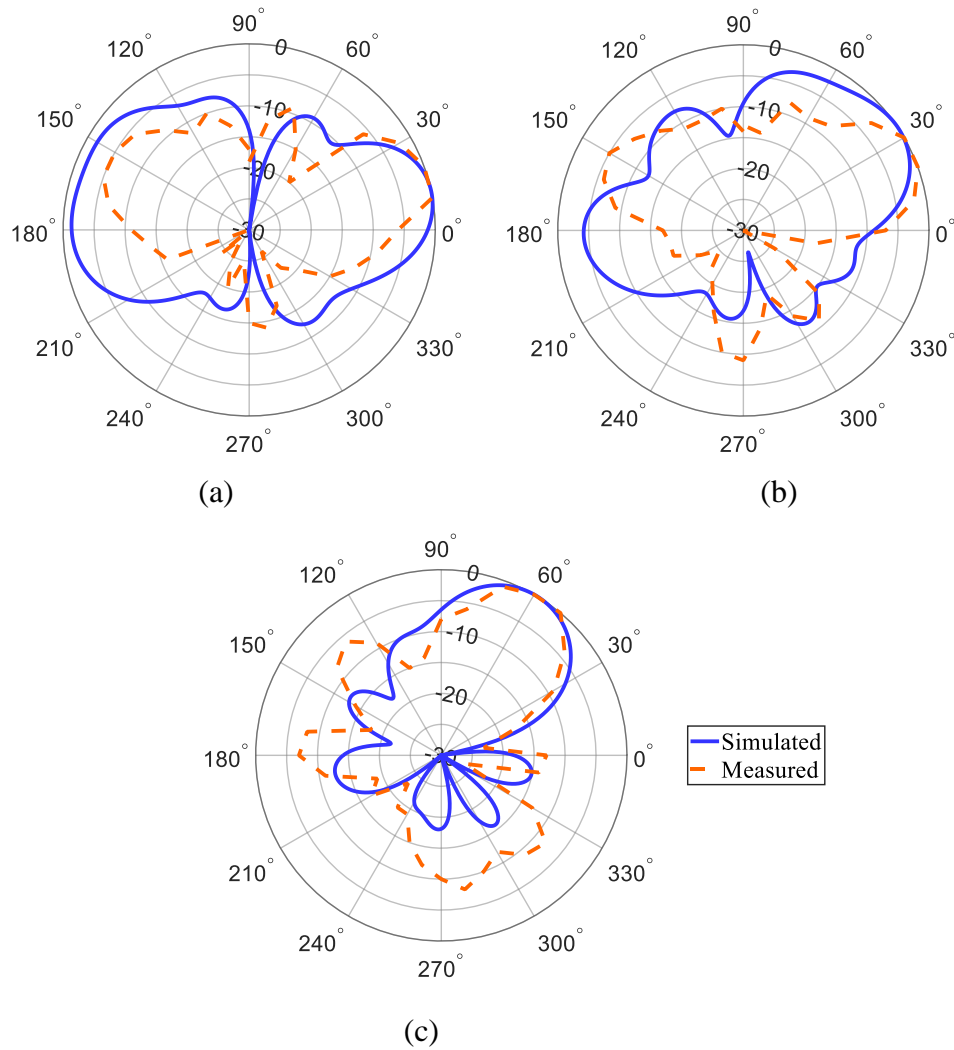


Figure 26 Results measured for (a) $\theta_0 = 10^\circ$, (b) $\theta_0 = 30^\circ$ and (c) $\theta_0 = 60^\circ$.

Table 8 shows the comparison of some intelligent antenna array technologies that use electrical excitation mechanisms to control the radiation diagram. The system presented has full

angular coverage and no significant secondary lobes. Additionally, the proposed method allows the manipulation of phase and amplitude by an intelligent search PSO algorithm in order to find independent and optimized parameters to excite the arrays in each desired direction.

Table 8 Comparison between intelligent antenna arrays.

Reference	Technology	Specifications					
		Freq [GHz]	Angular Coverage	Significant Secondary Lobes	Power Control		
					Phase	Amplitude	Method
[8]	10th Linear Isotropic Elements	-	360°	Yes	Yes	Yes	Binomial and Chebyshev Polynomials
[35]	6th Dipole Switched Parasitic Array	3.5	60° sector	No	Yes	No	Genetic Algorithm (GA)
[36]	4th Dipoles in Linear Arrangement	2.16	180° sector	Yes	Yes	No	Dynamic Adjustment (Buttler Matrix)
This work	3 sets of 4 Yagi-Uda in Linear Arrangement	0.46	360°	No	Yes	Yes	PSO

To numerically compare the advantages of the scheme proposed for application in electrical distribution, a typical BTS radiating a signal at 459 MHz with power of 40 dBm was considered, covering a circular area of radius R . In addition, it was considered that remote devices connected to a gain antenna of 8 dBi are placed at the edge of this circle. For the traditional collinear array (6 dBi), applying the Friis equation [19] in an ideal situation where the BTS and the remote devices are at the same height and there is no obstacle between them, the remote devices receive a power of -53.77 dBm, at a distance equal to $R = 9$ km from the BTS. On the other hand, with the proposed scheme, the gain of the Yagi-Uda array varies between 10.13 and 13.31 dBi. For this new scenario, in the worst case, where the gain is 10.13 dBi, a remote device receives the same power of -53.77 dBm at an additional distance of $R =$

14.48 km. Therefore, comparing the two situations, the array of Yagi-Uda antennas covers a larger area (659.7km^2) than the Collinear Array (254.46 km^2). In practical terms, 36 BTSs with traditional Collinear Arrays would cover an area of $9,160.56\text{ km}^2$. Using the proposed Antenna Array to cover the same area, only 14 BTSs with Yagi-Uda Array are required, implying a 61% reduction in the number of BTSs needed for the same coverage.

6.4 OPTIMIZATION OF THE GEOMETRIC CONFIGURATION OF THE SMART ARRAY

In order to reduce the physical dimensions of the Antenna Array in the BTS, other geometric configurations of the arrays can be evaluated to ensure a coverage of 180° for each array, reducing from 3 to 2 Antenna Arrays per BTS.

As preliminary tests, the antennas at the ends of the array undergone an angular opening of 70° , as shown in Figure 27 and Figure 28. Table 9 presents the technical specifications of the Yagi-Uda antenna used in the final array and Figure 29, the applied antenna design.

Table 9 Technical characteristics of the antenna used in the intelligent array.

Features	Min.	Tip.	Max.	Unit
Operating Range	440		470	MHz
Number of Elements		7		
Reference		Y4460111-07SG(A-02)		
Manufacturer		TSM		
Nominal gain		11,4		dBi
Front-coast relationship		24		dB

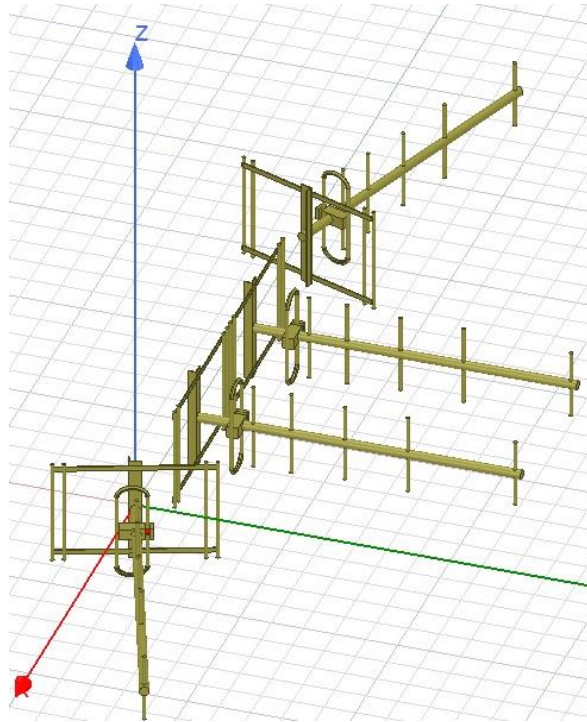


Figure 27 New geometric configuration for intelligent antenna array.

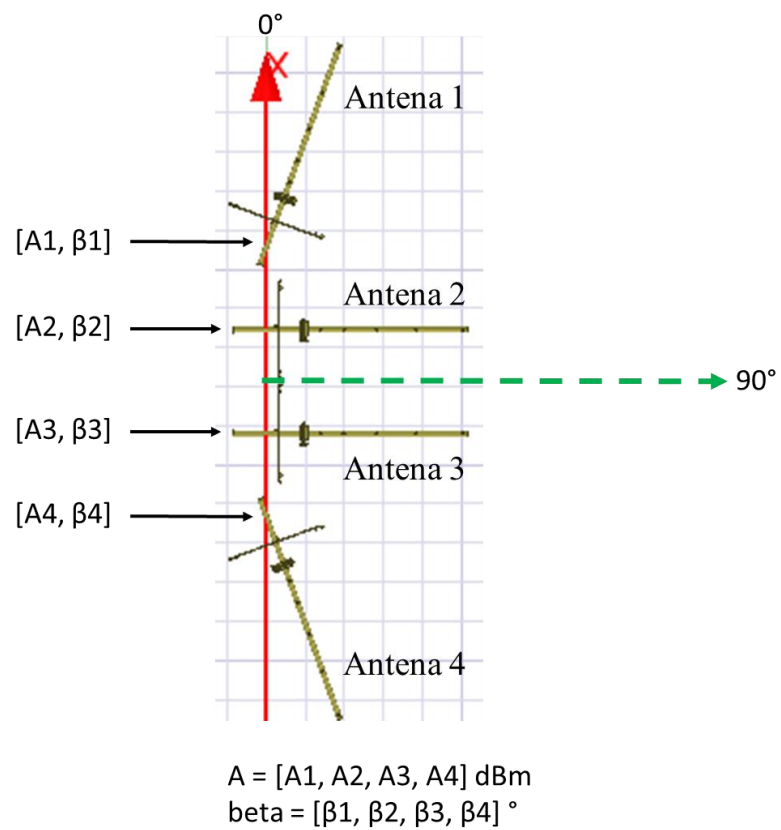


Figure 28 New geometric configuration for intelligent antenna array (superior view).

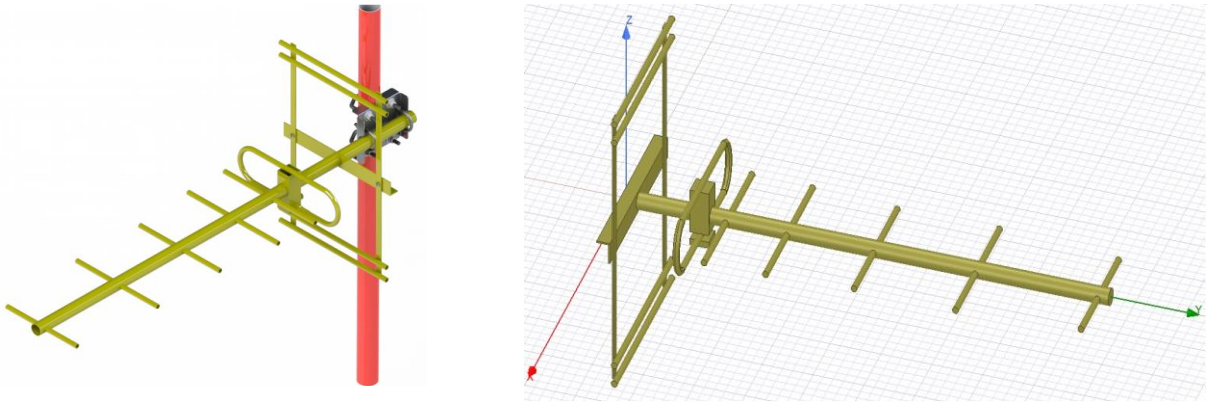


Figure 29 7-element Yagi-Uda antenna of the final configuration with grid reflector element. a) Photo present in the datasheet; b) Drawing of the antenna reproduced in the HFSS from its measurements.

In initial simulations for this new geometry, the results obtained show that this new configuration allows a coverage of 180° with gains between 10.64dBi and 14.15dBi. In this way, it would be feasible to reduce the BTS configuration with 360° coverage from 3 to 2 Smart Arrays in the *Back to Back configuration*. Figure 30 to Figure 36 show the radiation diagrams of this new configuration with an angular coverage variation of 15° .

Table 10 shows the Amplitudes and Excitation Phases applied to the diagrams of Figure 30 to Figure 36.

Table 10 Excitation settings applied to the antennas to obtain the diagrams of Figure 30 to Figure 36.

Direction	Excitements	
	Amplitudes (dBm)	Phases ($^\circ$)
0°	[26.29, 9.38, 12.40, 12.57]	[0.00, 221.46, 190.57, 69.02]
15°	[29.77, 14.14, 12.61, 18.44]	[0.00, 52.92, 52.92, -77.69]
30°	[29.90, 11.28, 17.07, 19.14]	[0.00, 303.36, 268.50, 118.59]
45°	[30.00, 28.75, 27.73, 17.80]	[0.00, -133.18, -197.42, 5.70]
60°	[16.80, 27.18, 24.85, 3.87]	[0.00, -236.77, -104.61, -40.05]
75°	[13.85, 24.38, 27.68, 11.83]	[0.00, 285.46, 347.13, 267.21]
90°	[-inf, 30.00, 30.00, -inf]	[0.00, 0.00, 0.00, 0.00]

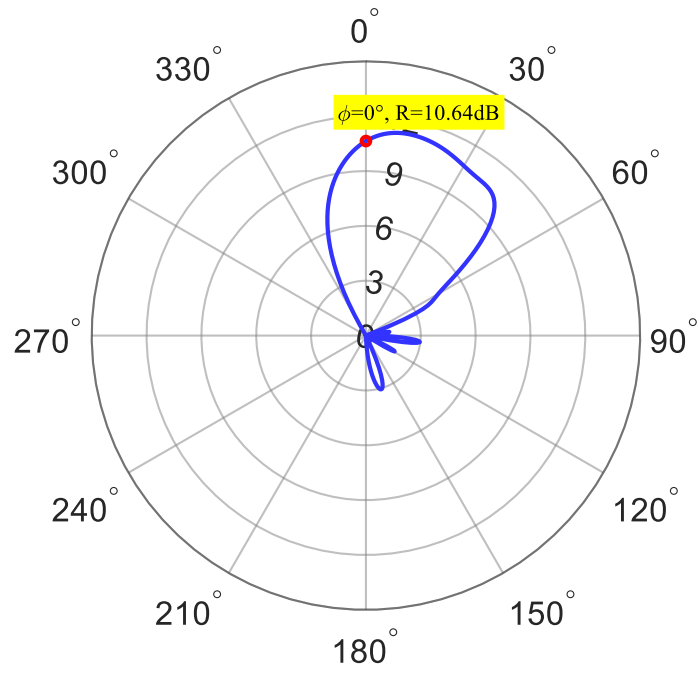


Figure 30 Radiation diagram for new configuration with $\theta_0 = 0^\circ$. Gain of 10.64dBi.

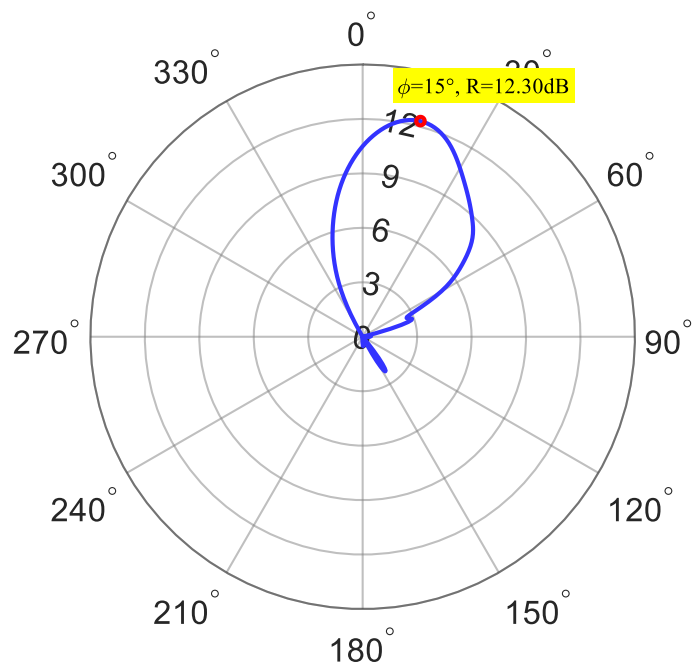


Figure 31 Radiation diagram for new configuration with $\theta_0 = 15^\circ$. Gain of 12.30dBi.

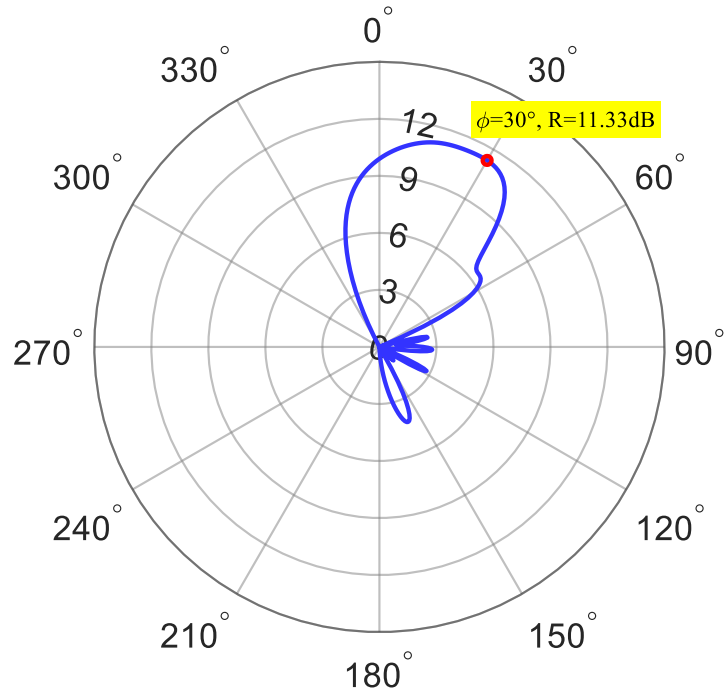


Figure 32 Radiation diagram for new configuration with $\theta_0 = 30^\circ$. Gain of 11.33dBi.

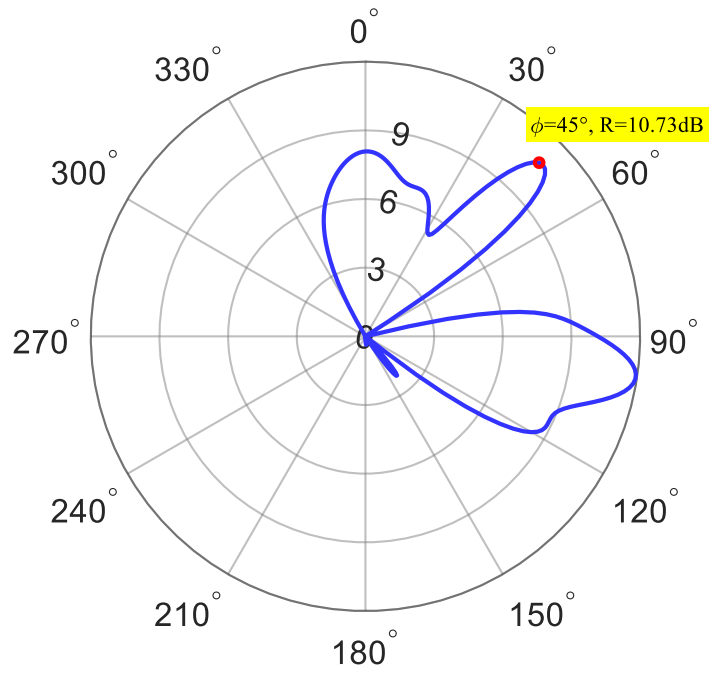


Figure 33 Radiation diagram for new configuration with $\theta_0 = 45^\circ$. Gain of 10.73dBi.

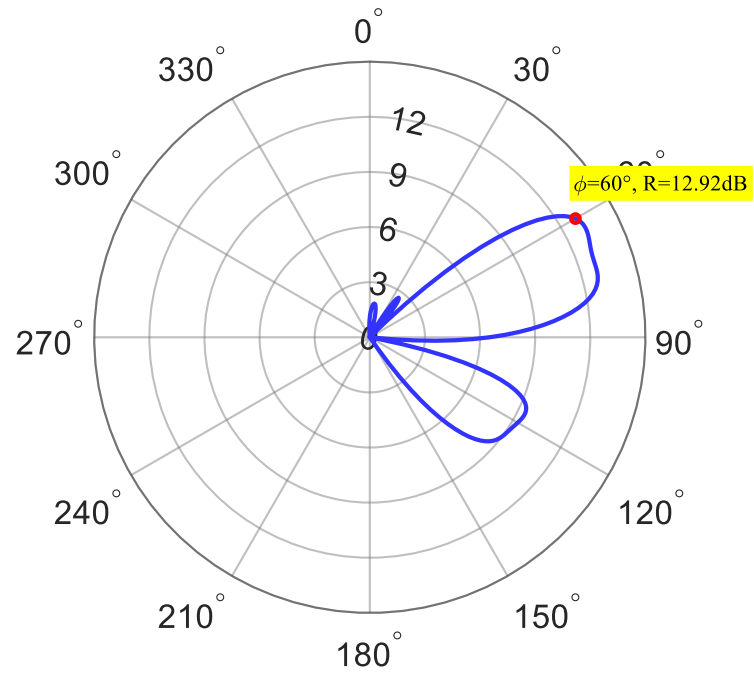


Figure 34 Radiation diagram for new configuration with $\theta_0 = 60^\circ$. Gain of 12.92dBi.

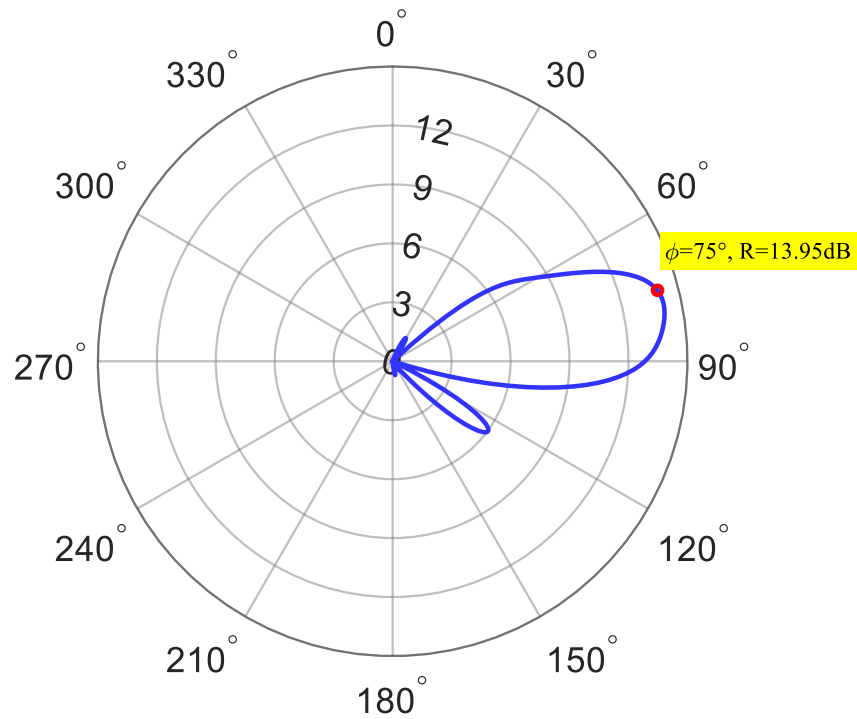


Figure 35 Radiation diagram for new configuration with $\theta_0 = 75^\circ$. Gain of 13.95dBi.

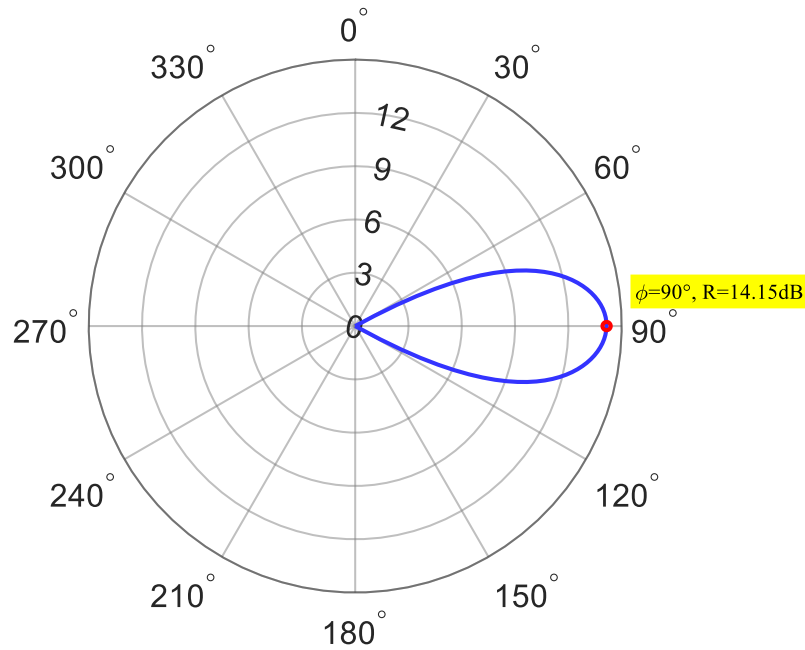


Figure 36 Radiation diagram for new configuration with $\theta_0=90^\circ$. Gain of 14.15dBi.

As can be observed in the radiation diagrams of Figure 30 to Figure 36, in the directions of interest, the gains of the signals were always greater than 9 dBi, which represents better results than those obtained when the antennas were parallel to each other (and did not have grid reflective elements).

For this new configuration, the control system would now have a controlled so turning system for 2 Antenna Arrays, as shown in Figure 37.

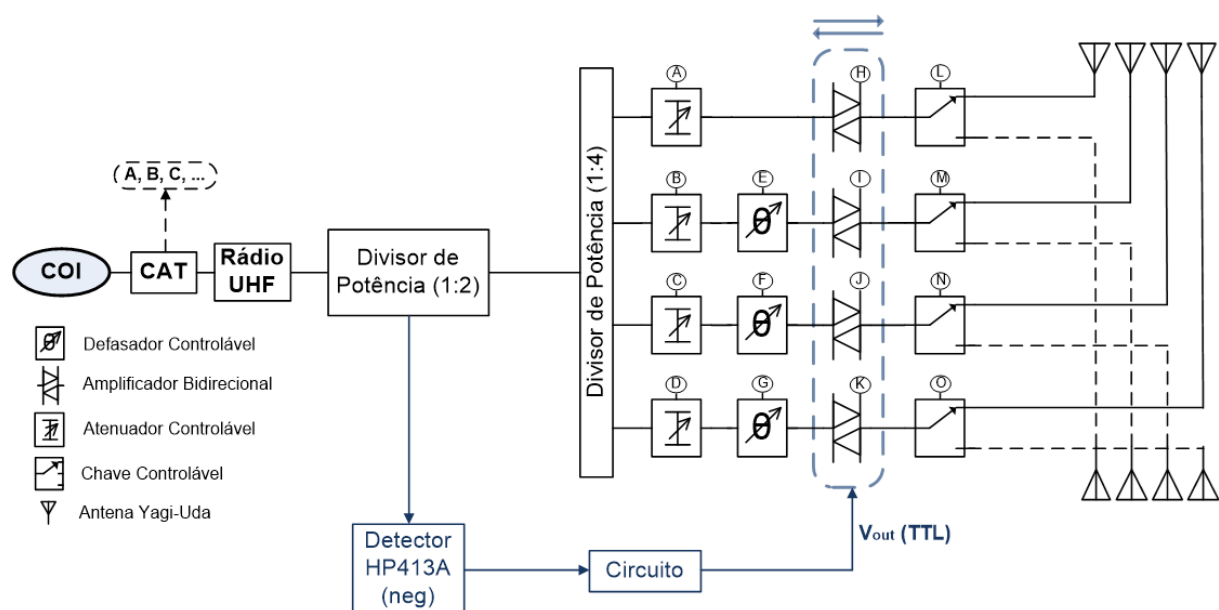


Figure 37 Complete system configuration for two antenna arrays.[6]

7 CONCLUSIONS

This work brought an innovation for the application in the electric energy sector, since the companies in the electric sector use as a transmitting antenna in their base stations, omnidirectional arrays, wasting the power radiated uniformly and having a smaller coverage area for the same power of the transmitter radio, which is limited regularly. As discussed in the Chapter 6, the intelligent antenna model brings a 61% reduction in the number of BTS to the same coverage area compared to the traditional omnidirectional array.

Another innovation of this work was the application of electronically controlled devices, addressed in Chapter 5. This allowed them to be encapsulated in an electronically controlled standard 19" cabinet, as shown in Figure 11. As mentioned in Chapter 4, this research is an evolution of a first stage of intelligent control of an antenna array, where devices with non-digital controls were applied in addition to the innovation of the method of defining the optimized parameters to obtain the maximum power density of the RF signal in the desired direction.

It has been shown that it is possible to automatically control the radiation diagram of the array according to the geographic coordinates of the transmitter and receiver, radiating the maximum power density to the devices connected to the communication link. The proposed optimized mathematical model is capable of feeding the array of antennas with the appropriate amplitude weights and excitation phases to generate a concentrated radiation lobe, allowing an efficient total coverage of 360°.

The optimization algorithm ensures, at a low computational cost, an optimal solution without producing considerable secondary lobes in undesirable directions, which would force the system to share the output diagram's density power with regions other than that of interest. This allows the signal strength in the desired direction to be amplified to the maximum, resulting in a greater range of the radiated signal.

7.1 SUGGESTIONS FOR FUTURE WORK

In order to improve the optimization methodology for estimating the parameters of the smart antenna array, we propose the development of an estimation methodology using the concepts of neural networks.

The neural system, with an input related to the geographic coordinates of the network equipment (recloser) and the Base Radio Station, would have as output the optimized parameters estimated for the maximum power of the BTS in the desired direction. The input

of the neural system can also be the angle from which the maximum power density is to be directed. The output of the system are the 4 weights and the 4 electrical phases that will give the maximum gain in the desired direction.

Figure 38 illustrates the configuration of the method to be addressed in the future.

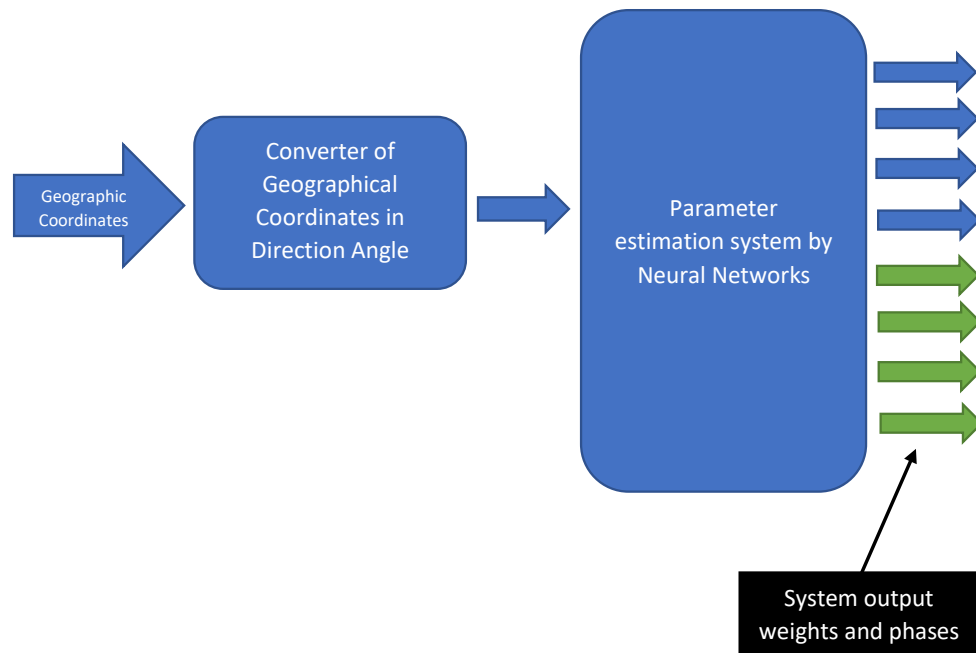


Figure 38 Proposal of a model for estimating the parameters of the intelligent array using neural networks.

7.2 CONTRIBUTIONS AND SCIENTIFIC PRODUCTION

As contributions generated by the studies carried out in the realization of this doctorate, the results presented in this thesis produced, directly or through collaborations developed in the microwave laboratory of UFPE, the set of scientific publications listed below, which includes an article published in a journal with a high impact factor and several papers accepted at important international conferences in the area.

7.2.1 Papers published in journals

1. **B. A. Kleinau**, D. L. de Melo, M. T. de Melo, D.C. P. Barbosa, A. J.B. Oliveira, C. P. N. Silva, and J.M. A.M. de Oliveira, "Application of the Base Transceiver Station with

Smart Antennas in the Power Distribution Sector", International Journal of Antennas and Propagation, vol. 2021, Article ID 6621116. View at: <https://www.hindawi.com/journals/ijap/2021/6621116/>

2. J. M. A de Oliveira, D. L. de Melo, C. P. do N. Silva, A. J. Belfort de Oliveira, A. F. L. Alves da Silva, A. Gomes Barboza, D. de Filgueiras Gomes, M. T. de Melo, B. A. Kleinau, R. J. F. P. V. de Almeida, "Control and Optimization of a Smart Antenna Array by PSO", International Journal of Applied Electromagnetics and Mechanics.

7.2.2 Chapters of published books

1. OLIVEIRA, E.M. F.; OLIVEIRA, M. R. T.; De Oliveira B.G.M.; melo, M. T.; **KLEINAU**, B. A. Beam Trainer for Array of UHF Antennas with Application in Supervision of Electrical Networks. In: José Temístocles Ferreira Júnior; Renata Barbosa Vicente; Suzana Ferreira Paulino Domingos; Cecilia Maria Mota Silva Lins; Raphael Leite de Andrade Reis; Tereza Raquel Brito de Melo Conde. (Org.). Research, Extension, Citizenship and Social and Academic-Scientific Developments at UFRPE - Academic Unit of Cabo de Santo Agostinho - UACSA. 1ed. Recife: EDUFRPE, 2021, v. 02, p. 121-136.

7.2.3 Papers published in conference editorials

1. **Kleinau, B.A.**; Queiroz, S.; Padilha, R.; De Melo, M. T., "Communication System Using an Intelligent Antenna Array", 2019 UTC Latin America Summit 2019, Rio de Janeiro.
2. **Kleinau, B.A.**; Queiroz, S.; Padilha, R.; De Melo, M. T.; Oliveira, E.M. F., "Back-to-back double antenna array with 360° coverage simulation model," *2019 SBMO/IEEE MTT-S International Microwave and Optoelectronics Conference (IMOC)*, Aveiro, in press.
3. J.M.A.M. Oliveira, C. P. Do N. Silva, D. L. de Melo, J. P. R. Carvalho, D. L. S. Do Nascimento, J. P.B da Silva, D. De F. Gomes, A.J.B. de Oliveira, M.T. de Melo, **B. A. Kleinau** and R. J. F. P. V. de Almeida, " Chave SPDT por ressoadores acoplados de malha aberta para a banda de UHF", MOMAG 2020 (19° SBMO - Brazilian Symposium on Microwaves and Optoelectronics and the 14th CBMag - Brazilian Congress of Electromagnetism), Niterói.

4. D. L. de Melo, D. L. S. do Nascimento, M. T. de Melo, **B. A. Kleinau**, C. P. do N. Silva, A. F. L. Alves da Silva, D. de Filgueiras Gomes, J.M. A de Oliveira, A. Gomes Barboza, A. J. Belfort de Oliveira and R. J. F. P. V. de Almeida, "Optimization of an array of smart antennas using PSO for the monitoring of electrical power switches", 2020 IEEE MTT-S Latin America Microwave Conference (LAMC 2020), 2021, pp. 1-3, doi: 10.1109/LAMC50424.2021.9602041.

7.2.4 Patent application

1. M. T. de Melo, A. J. Belfort de Oliveira, D. de Filgueiras Gomes, C. P. do N. Silva, J. M. A de Oliveira, A. G. Barbosa, R. Padilha, B. A. Kleinau, "Sistema Inteligente Formador de Feixe, aplicado à Rede de Distribuição de Energia", BR1020140309373, 13 de Jun, 2022.

REFERENCES

- [1] M. T. de Melo, Propagação, Antenas e Projeto de Radioenlace, 1st ed., Recife, PE: Editora Universitária, 2007, pp. 92 - 98.
- [2] R. J. Mailloux, Phase Array Antenna Handbook, 2nd ed., Norwood, MA: Artech House, 2005, pp. 100-127.
- [3] L.C. Godara, "Applications of antenna arrays to mobile communications Part I. Performance improvement, feasibility, and system considerations," *Proc. IEEE*, vol. 85, p. 1031–1060, Jul. 1997.
- [4] H. S. a. H.B. Y. Harkouss, "Direction of arrival estimation for smart antenna in multipath environment using convolutional neural network," *Int. J. RF Microw. Comput. -Aided Eng*, vol. 28, n° 6, Aug. 2018.
- [5] R. G. Ayestaron, "Fast near-field multifocusing of antenna arrays including element coupling using neural networks," " *IEEE Antennas Wirel. Propag. Lett.*, vol. 17, no. 7, pp. 1233-1237, Jul. 2018.
- [6] B. G.M. d. Oliveira, "Switched smart antenna system for SCADA telesupervision and telecontrol systems," in *SBMO/IEEE MTT-S Int. Microw. Optoelectron. Conf., IMOC*, Rio de Janeiro, 2013.
- [7] M. A. BRANQUINHO, "Safety of Industrial Automation and SCADA," *Elsevier Brasil*, 2014.
- [8] C. A. BALANIS, Antenna theory: Analysis and design., 4th ed., New York: John Wiley & Sons, 2016, pp. 283-321.
- [9] D. K. Cheng, Field and Wave Electromagnetics, 2nd ed., Asia: Pearson, 2006, pp. 600-664.
- [10] T. A. Milligan, Modern Antenna Design, 2nd ed., New Jersey: John Wiley & Sons, 2005, pp. 485-497.
- [11] S. & K. G. Pandav, "Modeling of Yagi-Uda antenna using Method of Moments," *IETE Technical Review*, 17, pp. 283-291, 2015.
- [12] M. R. a.C. P. W. Ma, "The modelling of a Yagi-Uda array antenna using the DGF-FDTD method," at *IEEE Antennas and Propagation Society International Symposium*, Columbus, OH, 2003.
- [13] M. K. a.M. Al-Aqil, "Design and Optimization of Yagi-Uda antenna arrays," *IET Microwaves, Antennas & Propagation*, vol. 4, no. 4, pp. 426-436, April 2010.
- [14] S.M. T. a.M. V. T. H. E. R. Schlosser, "Particle swarm optimization for antenna arrays synthesis," *SBMO/IEEE MTT-S International Microwave and Optoelectronics Conference (IMOC)*, pp. 1-6, 2015.
- [15] B.-h. S. a. Q.-z. L. Jian-feng Li, "PSO-based optimization of broadband antenna array for space-division communication system," *8th International Symposium on Antennas, Propagation and EM Theory*, pp. 309-312, 2008.
- [16] J. K. a. R. Eberhart, "Particle swarm optimization," at *Proceedings of ICNN'95 – International Conference on Neural Networks*, Perth, Australia, 1995.
- [17] HFSS, "3D Electromagnetic Field Simulator for RF and wireless Design," 2020. [Online]. Available: <https://www.ansys.com/products/electronics/ansys-hfss>.
- [18] D. K. S. a. Z. J.C. J. J. F. Lee, "Tangential vector finite elements for electromagnetic field computation," *IEEE Transactions on Magnetics*, vol. 27, no. 5, pp. 4032-4035, September 1991.

- [19] R. F. Harrington, "The method of moments in electromagnetics," *Journal of Electromagnetic waves and Applications*, vol. 1, no. 3, pp. 181-200, 1987.
- [20] J.-S. Wang, "Finite element computation of antenna impedance including feed modeling," *IEEE Transactions on Magnetics*, vol. 33, no. 2, pp. 1500-1503, March 1997.
- [21] M. S. P.B. S. Munish Rattan, "Optimization of Gain, Impedance, and Bandwidth of Yagi-Uda Array Using Particle Swarm Optimization," *International Journal of Antennas and Propagation*, p. 4 pages, 2008.
- [22] E. A. J. a. W. T. Joines, "Design of Yagi-Uda antennas using genetic algorithms," *IEEE Transactions on Antennas and Propagation*, vol. 45, no. 9, pp. 1386-1392, September 1997.
- [23] L. A. e. a. Greda, "Beamsteering and beamshaping using a linear antenna array based on particle swarm optimization," *IEEE Access*, vol. 7, pp. 141562-141573, 2019.
- [24] X. e. a. Zhang, "Antenna array design by a contraction adaptive particle swarm optimization algorithm," *EURASIP Journal on Wireless Communications and Networking*, vol. 1, p. 57, 2019.
- [25] S. K. H. a. H.C. W. A. Ratnaweera, "Self-organizing hierarchical particle swarm optimizer with time-varying acceleration coefficients," *IEEE Transactions on Evolutionary Computation*, vol. 8, no. 3, pp. 240-255, June 2004.
- [26] S. X. a. Y. Rahmat-Samii, "Boundary Conditions in Particle Swarm Optimization Revisited," *IEEE Transactions on Antennas and Propagation*, vol. 55, no. 3, pp. 760-765, March 2007.
- [27] C. Han and L. Wang, "Array pattern synthesis using particle swarm optimization with dynamic inertia weight," *International Journal of Antennas and Propagation*, vol. 2016, 2016.
- [28] D. e. a. Liu, "Synthesis of unequally spaced antenna arrays by using inheritance learning particle swarm optimization," *Progress In S. ElectromagneticS Research*, vol. 118, pp. 205-221, 2011.
- [29] S. e. a. Huang, "Pipeline Implementation of Polyphase PSO for Adaptive Beamforming Algorithm," *Huang, Shaobing et al.*, , vol. 2017, 2017.
- [30] S. K. Goudos, C. Kalialakis and R. Mittra, "Evolutionary algorithms applied to antennas and propagation: A review of state of the art," *International Journal of Antennas and Propagation*, vol. 2016, 2016.
- [31] J. R. a. Y. Rahmat-Samii, "Particle swarm optimization in electromagnetics," in *IEEE Transactions on Antennas and Propagation*, vol. 52, no. 2, pp. 397-407, Feb. 2004.
- [32] Y.R.-S. Nanbo Jin, "Particle Swarm Optimization for Antenna Designs in Engineering Electromagnetics," *Journal of Artificial Evolution and Applications*, vol. 2008, p. 10 pages, 2008.
- [33] G. e. a. Sun, "An antenna array sidelobe level reduction approach through invasive weed optimization," *International Journal of Antennas and Propagation*, vol. 2018, 2018.
- [34] Python, "<https://www.python.org/>," 2015. [Online].
- [35] P. K. V. P. T. T. a.C. N.C. A. I. Sotiriou, "Broadband Wireless Access Base Station Performance using Smart Antenna Cell," in *2007 International workshop on Antenna Technology: Small and Smart Antennas Metamaterials and Applications*, Cambridge, 2007.

- [36] S. J. F. a. D. S. F. Bobor-Oyibo, "A multiple switched beam Smart antenna with beam shaping for dynamic optimisation of capacity & coverage in mobile telecommunication networks," at *8th International Symposium on Antennas, Propagation and EM Theory*, Kunming, 2008.